Vandeputte, Caroline and Reumers, Veerle and Aelvoet, Sarah-Ann and Thiry, Irina and De Swaef, Sylvie and Van den Haute, Chris and Pascual-Brazo, Jesus and Farr, Tracy D. and Vande Velde, Greetje and Hoehn, Mathias and Himmelreich, Uwe and Van Laere, Koen and Debyser, Zeger and Gijsbers, Rik and Baekelandt, Veerle (2014) Bioluminescence imaging of stroke-induced endogenous neural stem cell response. Neurobiology of Disease, 69 . pp. 144-155. ISSN 09699961

Bioluminescence imaging of stroke-induced endogenous neural stem cell response.

Caroline Vandeputte [a,b,c,¶]**, Veerle Reumers** [a,¶]**, Sarah-Ann Aelvoet** [a,¶]**, Irina Thiry** [d]**, Sylvie De Swaef** [a]**, Chris Van den Haute** [a,e]**, Jesus Pascual-Brazo** [a]**, Tracy D. Farr** [f]**, Greetje Vande Velde** [b,g]**, Mathias Hoehn** [f]**, Uwe Himmelreich** [b,g]**, Koen Van Laere** [b,c]**, Zeger Debyser** [b,d]**, Rik Gijsbers** [d,e,*]**, Veerle Baekelandt** [a,b,*]

a KU Leuven, Laboratory for Neurobiology and Gene Therapy, Department of Neurosciences, 3000 Leuven, Flanders, Belgium
b KU Leuven, Molecular Small Animal Imaging Center, MOSAIC, KU Leuven, 3000 Leuven, Flanders, Belgium
c Division of Nuclear Medicine, University Hospital and KU Leuven, 3000 Leuven, Flanders, Belgium
d KU Leuven, Laboratory for Molecular Virology and Gene Therapy, Department of Pharmaceutical and Pharmacological Sciences, 3000 Leuven, Flanders, Belgium
e KU Leuven, Leuven Viral Vector Core, 3000 Leuven, Flanders, Belgium
f In-vivo-NMR Laboratory, Max Planck Institute for Neurological Research, 50931 Cologne, Germany
g KU Leuven, Biomedical MRI, Department of Imaging and Pathology, 3000 Leuven, Flanders, Belgium

¶ shared first authors

* shared last authors

Keywords: Bioluminescence imaging/ Cre-Flex lentiviral vector/ Endogenous neural stem cells/Nestin-Cre mice/ Stroke

Address for correspondence:

Prof. Veerle Baekelandt, Laboratory of Neurobiology and Gene Therapy,

KU Leuven, Kapucijnenvoer 33, 3000 Leuven, Flanders, Belgium.

E-mail: Veerle.baekelandt@med.kuleuven.be

Abstract

Brain injury following stroke affects neurogenesis in the adult mammalian brain. However, a complete understanding of the origin and fate of the endogenous neural stem cells (eNSCs) in vivo is missing. Tools and technology that allow non-invasive imaging and tracking of eNSCs in living animals will help to overcome this hurdle. In this study, we aimed to monitor eNSCs in a photothrombotic (PT) stroke model using in vivo bioluminescence imaging (BLI). In a first strategy, inducible transgenic mice expressing firefly luciferase (Fluc) in the eNSCs were generated. In animals that received stroke, an increased BLI signal originating from the infarct region was observed. However, due to histological limitations, the identity and exact origin of cells contributing to the increased BLI signal could not be revealed. To overcome this limitation, we developed an alternative strategy employing stereotactic injection of conditional lentiviral vectors (Cre-Flex LVs) encoding Fluc and eGFP in the subventricular zone (SVZ) of Nestin-Cre transgenic mice, thereby specifically labeling the eNSCs. Upon induction of stroke, increased eNSC proliferation resulted in a significant increase in BLI signal between 2 days and 2 weeks after stroke, decreasing after 3 months. Additionally, the BLI signal relocalized from the SVZ towards the infarct region during the 2 weeks following stroke. Histological analysis at 90 days post stroke showed that in the peri-infarct area, 36% of labeled eNSC progeny differentiated into astrocytes, while 21% differentiated into mature neurons. In conclusion, we developed and validated a novel imaging technique that unequivocally demonstrates that nestin+ eNSCs originating from the SVZ respond to stroke injury by increased proliferation, migration towards the infarct region and differentiation into both astrocytes and neurons. In addition, this new approach allows non-invasive and specific monitoring of eNSCs over time, opening perspectives for preclinical evaluation of candidate stroke therapeutics.

Introduction

The presence of endogenous neural stem cells (eNSCs) in the adult mammalian brain, including human brain, is now widely accepted (Altman, 1962, 1963; Curtis et al., 2005; Eriksson et al., 1998). Two brain regions, i.e. the SVZ of the lateral ventricles and the subgranular zone (SGZ) of the hippocampal dentate gyrus, are recognized as primary regions of adult neurogenesis (Ming and Song, 2005). Under physiological conditions, eNSCs in the SVZ divide and their progeny migrates tangentially via the rostral migratory stream (RMS) to the olfactory bulb (OB). Upon arrival in the OB, neuroblasts differentiate into local interneurons and integrate into the glomerular and granular layers (Alvarez-Buylla and Garcia-Verdugo, 2002). Pathological conditions, including brain injury and stroke, affect adult neurogenesis (Curtis et al., 2005; Gray and Sundstrom, 1998; Liu et al., 1998). Stroke, a common cause of morbidity and mortality worldwide, deprives the brain of oxygen and glucose (Flynn et al., 2008). Following stroke, neurogenesis augments the number of immature neurons in the SVZ (Jin et al., 2001; Zhang et al., 2008). Neuroblasts (positive for the marker doublecortin, DCX) migrate towards sites of ischemic damage and upon arrival, phenotypic markers of mature neurons can be detected (Arvidsson et al., 2002; Parent et al., 2002). On the other hand, retroviral labeling of the SVZ showed that cells migrated to the lesion and differentiated into glia (Goings et al., 2004), demonstrating that following injury, the SVZ can generate both neural cell types. Some studies showed that SVZ-derived progenitors can differentiate into medium spiny neurons in the striatum after stroke (Collin et al., 2005; Parent et al., 2002), whereas others claimed that the newborn cells are fate restricted to interneurons or glia (Deierborg et al., 2009; Liu et al., 2009). Whether SVZ neural progenitors can alter their fate, integrate in the injured circuits and survive for long time periods is still a matter of debate (Kernie and Parent, 2010). Up till now, specific labeling of eNSCs in the SVZ and the follow-up of the migration of their progeny to the ischemic area over time has not yet been shown.

Apart from the primary neurogenic niches, other brain regions, e.g. the cortex, contain cells that become multipotent and self-renew after injury (Komitova et al., 2006). Although mature astrocytes do not divide in healthy conditions, they can dedifferentiate and proliferate after stab wound injury and stroke (Buffo et al., 2008; Sirko et al., 2013). While these proliferating astrocytes remained within their lineage in vivo, they formed multipotent neurospheres in vitro (Buffo et al., 2008; Shimada et al., 2010). Therefore, these reactive astrocytes may represent

87 an alternative source of multipotent cells that may be beneficial in stroke.

88

89 A major hurdle when studying endogenous neurogenesis is the lack of methods to monitor these

90 processes in vivo, in individual animals over time. We and others attempted to label eNSCs by

91 injection of iron oxide-based particles in the lateral ventricle or SVZ (Nieman et al., 2010;

92 Shapiro et al., 2006; Sumner et al., 2009; Vreys et al., 2010), or by lentiviral vectors (LVs)

93 encoding a reporter gene into the SVZ (Vande Velde et al., 2012) to monitor stem cell migration

94 along the RMS with magnetic resonance imaging (MRI). Although MRI provides high

95 resolution, it suffers from low in vivo sensitivity and gives no information on cell viability and

96 non-specific signal detection cannot be excluded. Rueger et al. described in vivo imaging of

97 eNSCs after focal cerebral ischemia via positron emission tomography (PET) imaging (Rueger et

98 al., 2010), however, the cells responsible for the PET signal could not be identified.

99 Alternatively, transgenic mice expressing Fluc driven by a DCX promoter allowed monitoring of

100 adult neurogenesis using in vivo BLI (Couillard-Despres et al., 2008). However, the robust BLI

101 signal emitted from the SVZ, leading to scattering and projection of these photons to the OB,

102 impedes direct visualization of eNSC migration from the SVZ towards the OB. Moreover, when

103 the DCX+ neuroblasts differentiate into mature neurons, they lose the Fluc expression. In a first

104 part of the present study, we generated inducible transgenic mice that express Fluc in the nestin+

105 eNSCs, to monitor a stroke-induced eNSC response with BLI.

106

107 An alternative strategy to efficiently and stably introduce Fluc in the eNSCs is by stereotactic

108 injection of LVs into the SVZ, which allowed us and others to monitor the migration of eNSCs

109 and their progeny towards the OB with BLI (Guglielmetti et al., 2013; Reumers et al.,

110 2008). However, since LVs transduce both dividing and post-mitotic cells, not only eNSCs but

111 also neighboring astrocytes and mature neurons are labeled after injection of constitutive LVs in

112 the SVZ (Geraerts et al., 2006). As a result, in line with the data described in transgenic mice, a

113 high BLI signal emerges from the site of injection that interferes with the measurement of the

114 migrating cells (Reumers et al., 2008). To overcome the latter, we developed new conditional

115 Cre-Flex LVs in a second part of this study. These Cre-Flex LVs incorporate Cre-lox technology,

116 allowing that Fluc and eGFP are restrictively expressed in eNSCs after injection in the SVZ of

117 transgenic Nestin-Cre mice. While numerous research groups have previously described

118 stroke-induced eNSC behavior (Arvidsson et al., 2002; Parent et al., 2002), we here report for the

119 first time successful in vivo imaging and characterization of long-term eNSC responses after

120 stroke.

121

122 **Materials & methods**

123

124 *Animals*

125

126 Animal studies were performed in accordance with the current ethical regulations of the KU

127 Leuven. Nestin-CreERT2 mice (a kind gift from Dr. Amelia J. Eisch (University of Texas

128 Southwestern Medical Center, Dallas, TX) (Lagace et al., 2007)) and B6.Cg-Tg(Nes-cre)1Kln/J

129 (Jax labs stock nr 003771, (Tronche et al., 1999)) were crossbred with C57BL/6-Tyrc-2J/J (Jax

130 labs, stock nr 000058), creating white furred albino mice in a C57BL/6 genetic background.

131 White furred inducible Nestin-CreERT2 mice were crossbred with ROSA26-LoxPstop-

132 LoxP(L-S-L)-luciferase transgenic mice (Safran et al., 2003) (Jax labs, stock nr 005125),

133 indicated as Nestin-CreERT2/Fluc mice. To induce Fluc expression, mice received tamoxifen

134 intraperitoneally (ip) or orally at 180 mg/kg dissolved in 10% EtOH/90% sunflower oil for 5

135 consecutive days. BrdU was administered as previously published (Geraerts et al, 2006). For the

136 stroke follow-up, Fluc expression was induced in 11 Nestin-CreERT2/Fluc mice by oral

137 tamoxifen treatment. Four days later, the animals were divided into 2 groups: 8 mice received a

138 PT stroke and 2 mice received a sham treatment; one mouse died during tamoxifen induction.

139 Three Cre-negative littermates that received a stroke were added as controls.

140

141 White furred B6.Cg-Tg(Nes-cre)1Kln/J mice, here referred to as Nestin-Cre mice, were

142 stereotactically injected with Cre-Flex LV in the SVZ at the age of 8 weeks. One week after

143 stereotactic injection, Nestin-Cre mice received a PT stroke (n = 33) or sham treatment

144 (n = 10). A Cre-negative littermate that received a stroke was added as control.

145

146 Mice were genotyped by PCR using genomic DNA and primers previously described (Lagace et

147 al., 2007).

148

149 *Lentiviral vector construction and production*

150

151 We designed a new conditional LV system based on the Cre/loxP mechanism, here referred to as

152 Cre-Flex (Cre-mediated flip-excision). The Cre-Flex LVs carry a reporter cassette encoding GFP

153 and Fluc flanked by a pair of mutually exclusive lox sites. The reporter cassette is activated after

154 Cre recombination (flip-excision, Fig. 3A). For the construction of the Cre-Flex plasmids,we

155 used the pCHMWS-eGFP plasmid as a backbone (Geraerts et al., 2006). As illustrated in Fig.

156 3A, pairs of heterotypic loxP_loxm2 recombinase target sites were cloned respectively, upstream

157 and downstream of eGFP using synthetic oligonucleotide adaptors. To enable efficient

158 recombination, 46-bp spacers were inserted in between both lox sites. In this plasmid, eGFP was

159 replaced by the coding sequence for eGFP-T2A-Fluc (Ibrahimi et al., 2009). All cloning steps

160 were verified by DNA sequencing. Cre-Flex LVs were generated and produced by the Leuven

161 Viral Vector Core essentially as described previously (Geraerts et al., 2005; Ibrahimi et al.,

162 2009). Before the start of the in vivo experiments, the LV-Cre-Flex was validated in cell

163 culture (Supplementary Fig. 1).

164

165 *Lentiviral vector injections*

166

167 Mice were anesthetized by ip injection of ketamine (75 mg/kg; Ketalar, Pfizer, Brussels,

168 Belgium) and medetomidin (1 mg/kg; Domitor, Pfizer), and positioned in a stereotactic head

169 frame (Stoelting, Wood Dale, Illinois, USA). Using a 30-gaugeHamilton syringe (VWR

170 International, Haasrode, Belgium), 4 μL of highly concentrated Cre-Flex LV was

171 injected in the SVZ at a rate of 0.25 μL/min. After injection of 2 μL, the needle was raised

172 slowly over a distance of 1 mm. After injection of the total volume the needle was left in place

173 for an additional 5min to allow diffusion before being slowly redrawn from the brain. SVZ

174 injections were performed at the following coordinates relative to Bregma: anteroposterior

175 0.5 mm, lateral−1.5 mm and dorsoventral−3.0–2.0 mm. After surgery, anesthesia was reversed

176 with an ip injection of atipamezol (0.5 mg/kg; Antisedan, Orion Pharma, Newbury, Berkshire,

177 UK).

178

179 *Stroke models*

180

181 Anesthesia was provided with 2% isoflurane/O2 gas anesthesia (Halocarbon Products

182 Corporation, New Jersey, USA) through a facemask. The PT strokes were induced according to

183 Vandeputte et al. (2011). Briefly, a vertical incision was made between the right orbit and the

184 external auditory canal. Next, the scalp and temporalis muscle were retracted. After intravenous

185   (iv) injection of the photosensitizer rose Bengal (20 mg/kg; Sigma Aldrich, St Louis, USA)

186   through the tail vein, photoillumination was performed for 5 min. Photoillumination

187   with green light (wave length, 540 nm; band width, 80 nm) was achieved using a xenon lamp

188   (model L-4887; Hamamatsu Photonics, Hamamatsu City, Japan) with heat-absorbing and green

189   filters. The irradiation at intensity 0.68 W/cm2 was directed with a 3-mm optic fiber, the head of

190   which was placed on the sensory motor cortex. Focal activation of the photosensitive dye

191   resulted in local endothelial cell injury leading to microvascular thrombosis and circumscribed

192   cortical infarctions (Watson et al., 1985). Sham-operated animals underwent the exact same

193   procedure as the animals with a stroke, except for the 5 min photoillumination.

194

195   Transient occlusion of the middle cerebral artery (MCA) was done using the intraluminal

196   filament technique previously described (Dirnagl and members of the MCAO-SOP group, 2009),

197   although in our experiments the MCA was occluded for 20 min.

198

199   *MR imaging*

200

201   For MRI data acquisition, mice were anesthetized with isoflurane (Halocarbon) in O2 (2.5% for

202   induction, 1.5–2% for maintenance). MR images were acquired using a Bruker Biospec 9.4 Tesla

203   small animal MR scanner (Bruker BioSpin, Ettlingen, Germany; horizontal bore, 20 cm) using a

204   cross-coil setup consisting of a 7.2 cm linearly polarized resonator for transmission and a mouse

205   head surface coil for signal reception as described before (Oosterlinck et al., 2011; Vandeputte et

206   al., 2011). In brief, the following protocols were used: (a) T2 maps using a MSME sequence

207   (10 echoes with 10 ms spacing, first TE=10 ms, TR=2000 ms, 16 interlaced slices of 0.4 mm,

208   100 μm2 in plane resolution); (b) T2-weighted MRI using a RARE sequence (TEeff = 71ms, TR

209   = 1300 ms, 100 μm3 isotropic resolution) and (c) high-resolution T2*-weighted 3D FLASH (TR

210   = 100 ms, TE = 12 ms, 100 μm3 isotropic resolution). The location of the needle tract after

211   stroke was measured with the Bruker Biospin software Paravision 5.x.

212

213   *In vivo bioluminescence imaging*

214

215   The mice were imaged in an IVIS 100 system (PerkinElmer, Waltham, MA, USA). Anesthesia

216   was induced in an induction chamber with 2% isoflurane in 100% oxygen at a flow rate of 1

217   L/min and maintained in the IVIS with a 1.5%mixture at 0.5 L/min. Before each imaging

218   session, the mice were injected iv with 126 mg/kg D-luciferin (Promega, Leiden, the

219   Netherlands) dissolved in PBS (15 mg/mL). Next, they were positioned in the IVIS and

220   consecutive 1 or 2min (depending on the experiment) frames were acquired until the maximum

221   signal was reached. Data are reported as the total flux (p/s/cm2/sr) from a specific region of

222   interest (ROI) of 12.5 mm2.

223

224   *Ex vivo bioluminescence imaging*

225

226   Immediately after in vivo BLI imaging, mice were sacrificed by cervical dislocation, decapitated

227   and the brain was dissected. The brain was placed in an acrylic brain matrix (Harvard apparatus,

228   Holliston, MA, USA) and sliced in 1.0 mm-thick sections. Next, these sections were imaged for

229   1 min in the IVIS.

230

231   *Immunohistochemistry*

232

233   Animals were sacrificed with an ip overdose (15 μL/g) of pentobarbital (Nembutal, CEVA Santé

234   Animale, Libourne, France) and transcardially perfused with 4% paraformaldehyde (PFA) in

235   PBS. Brains were removed and postfixed for 24 h with PFA. 50 μm thick coronal sections were

236   treated with 3% hydrogen peroxide and incubated overnight with the primary antibody, rabbit

237   anti-eGFP (made in-house, 1:10000 (Baekelandt et al., 2003)) or a rabbit anti-Cre recombinase

238   (1:3000 (Lemberger et al., 2007)), in 10% normal swine serum and 0.1% Triton X-100. The

239   sections were then incubated in biotinylated swine anti-rabbit secondary antibody (diluted 1:300;

240   Dako, Glostrup, Denmark), followed by incubation with streptavidin horseradish peroxidase

241   complex (Dako). Immune-reactive cells were detected by 3,3′-diaminobenzidine, using H2O2 as

242   a substrate. For 5-bromo-2′-deoxyuridine (BrdU) detection, sections were pre-treated for 30 min

243   in 2 N HCl at 37 °C, blocked in 0.1 M borate buffer for 20 min, rinsed 3 x 10 min in PBS before

244   incubation with rat anti-BrdU (1:400, Accurate chemical, NY, USA) in 10% horse serum,

245   followed by incubation with biotinylated donkey anti-rat secondary antibody (Jackson

246   ImmunoResearch Laboratories). The number of eGFP+ cells was estimated with an unbiased

247   stereological counting method, by employing the optical fractionator principle in a computerized

248   system, as described previously (Baekelandt et al., 2002) (StereoInvestigator, MicroBright-Field,

249   Magdeburg, Germany).

250

251   For immunofluorescent stainings, sections were treated with PBS-10% horse serum-0.1% Triton

252   X-100 for 1 h. Next, sections were incubated overnight at 4 °C in PBS–0.1% Triton X-100 with

253   the following antibodies: chicken anti-eGFP (1:500, Aves labs, Tigard, OR) and rabbit anti-glial

254   fibrillary acidic protein (GFAP) for astroglial cells and type B cells (1:500, Dako), goat anti-

255   doublecortin (DCX) for migrating neuroblasts (1:200, Santa Cruz Biotechnology), or rabbit anti-

256   neuronal nuclei (NeuN) for mature neurons (1:1000, EnCor Biotechnology Inc., Gainesville, FL,

257   USA). The next day, sections were incubated with the appropriate mixture of the following

258   fluorescently labeled secondary antibodies at room temperature for 2 h: donkey anti-chicken

259   (FITC, 1:200, Jackson Immuno Research Laboratories), donkey anti-goat (Alexa 555, 1:400,

260   Molecular Probes) or donkey anti-rabbit (Alexa 647, 1:400, Molecular Probes). Next, the

261   sections were washed in PBS- 0.1% Triton X-100 and mounted with Mowiol. Fluorescence was

262   detected with a confocal microscope (FV1000, Olympus) with a 488 nm, a 559 nm and a 633 nm

263   laser. The signal from each fluorochrome was collected sequentially. For the quantification of

264   double and triple positive cells, all GFP+ cells in the right SVZ, corpus callosum and stroke

265   region (one section per animal) were analyzed at 40X using z-plane confocal microscopy with 1

266   μm steps. All images shown correspond to projections of 18 μm z-stacks, except Fig. 6F which is

267   a single focal plane. Brightness, contrast and background were adjusted equally for the entire

268   image using 'brightness and contrast' controls in Image J.

269

270   *Statistics*

271

272   All statistical analyses were performed in Prism 5.0 (GraphPad Software). The statistical tests

273   that were used are indicated in the figure legends. Data are represented as mean ± standard error

274   of the mean (s.e.m.). p-values are indicated as follows: *p b 0.05, **p b 0.01, and

275   ***p b 0.001.

276

Results

Nestin-CreERT2/Fluc mice show an increased BLI signal after stroke

To monitor a stroke-induced eNSC response with BLI we initially used a transgenic strategy, where Nestin-CreERT2 mice were crossbred with ROSA26-loxP-stop-loxP(L-S-L)-luciferase transgenic mice. In the resulting Nestin-CreERT2/Fluc mice, Fluc expression is induced specifically in the nestin+ eNSCs following administration of tamoxifen (Lagace et al., 2007). First, we monitored the migration of eNSC progeny from the SVZ to the OB with BLI in healthy adult Nestin-CreERT2/Fluc mice. BLI was performed 1 week before and 1, 4, 8, 15 and 20 weeks after tamoxifen administration in healthy Nestin-CreERT2/Fluc mice (n = 5) or Cre-negative littermates (n= 4). At all time points investigated, no distinct in vivo BLI signals could be detected in the neurogenic regions of Nestin-CreERT2/Fluc mice and in Cre-negative littermates (Figs. 1A–C). Furthermore, there was no significant increase in BLI signal originating from the OB over time in Nestin-CreERT2/Fluc mice (Figs. 1 B,C). Although no differences in *in vivo* BLI signal could be detected, *ex vivo* BLI analysis showed a 2 to 3 fold higher BLI signal in the OB and SVZ of Nestin-CreERT2/Fluc mice compared to Cre-negative littermates (Figs. 1D,E). This indicates that Fluc is indeed expressed in eNSCs of the SVZ and in the progeny arriving in the OB, as is evidenced by ex vivo BLI, but the number of labeled cells is too low for in vivo detection. The latter might be explained by a low neurogenic potential in the Nestin-CreERT2/Fluc mice, since differences in neurogenic potential between mouse strains have been described (Kempermann et al., 1997). Therefore, we evaluated the neurogenic potential in Nestin-CreERT2/Fluc mice and in age matched C57BL/6 mice using BrdU (Supplementary Fig. 2) and showed that proliferation in the SVZ and number of newborn neurons arriving in the OB was not different. In conclusion, neurogenesis in SVZ and migration to the OB could not be monitored with in vivo BLI in healthy adult Nestin-CreERT2/Fluc mice.

Next, we investigated whether stroke-induced neurogenesis could be monitored in Nestin CreERT2/Fluc mice. Nine days after tamoxifen administration, mice either received a PT stroke in the right sensorimotor cortex (n=8) or a sham treatment (n=2) (Fig. 2A). Cre-negative littermates with stroke were included as controls (n = 3). BLI was performed one day prior to and

10
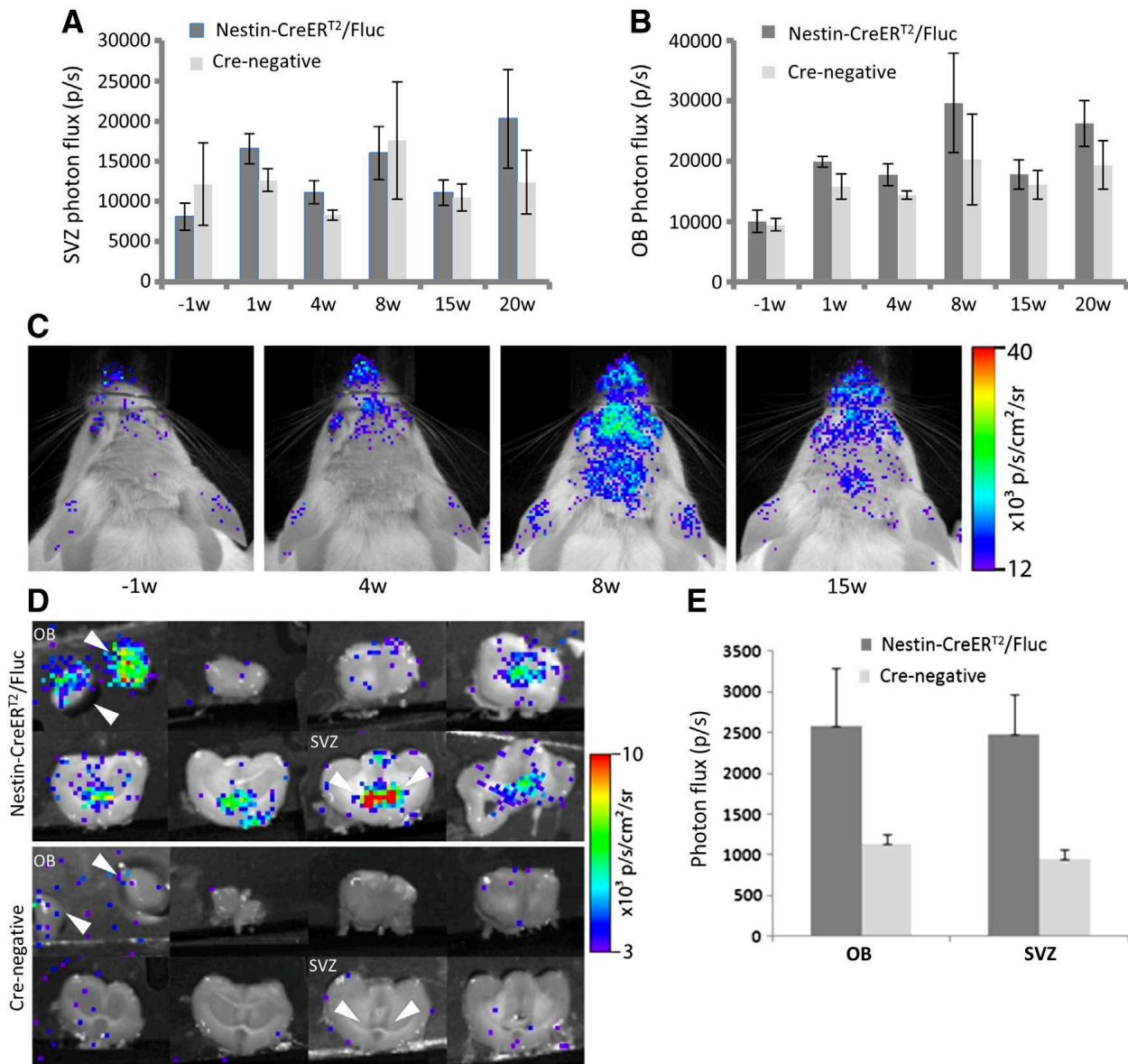
Fig. 1. Long-term follow-up of Nestin-CreERT2/Fluc mice with BLI. (A,B) A long-term follow-up of the BLI signal originating from the neurogenic brain regions was performed in Nestin-CreERT2/Fluc mice (n = 5) and Cre-negative littermates (n = 4). BLI was performed 1 week before and 1, 4, 8, 15 and 20 weeks after ip administration of tamoxifen. The BLI signal originating from the SVZ (A) and OB (B) was not significantly different from the background signal in Cre-negative littermates. Furthermore, no increase in BLI signal originating from the OB was detected over time (B). (C) BLI images of a representative Nestin-CreERT2/Fluc mouse 1 week before and 4, 8 and 15 weeks after tamoxifen administration. (D) Ex vivo BLI 20 weeks after induction shows a higher signal in the neurogenic regions in Nestin-CreERT2/Fluc mice compared to Cre-negative littermates. (E) Quantification of ex vivo BLI signals at 20 weeks shows a 2 to 3 fold higher signal emitted from the SVZ and the OB in the Nestin-CreERT2/Fluc mice compared to Cre-negative littermates.

11

322 7, 15, 22 and 33 days after surgery. In Nestin-CreERT2/Fluc mice receiving sham treatment and

323 in Cre negative littermates receiving stroke, no in vivo BLI signal could be detected (Figs.

324 2B,C). However, in 6 out of 8 Nestin-CreERT2/Fluc mice that received a stroke, a distinct BLI

325 signal emerging from the stroke area was detected starting at day 7 (Figs. 2B,C), compared to the

326 baseline scan before surgery, being 3.2 ± 0.4 fold higher at 7 days (p b 0.001), 4.2 ± 0.5 fold

327 higher at 15 days (p b 0.001), 2.1 ± 0.4 fold higher at 22 days (p b 0.05) and 1.9 ± 0.3 fold higher

328 at 33 days (not significant) after surgery (Fig. 2B). Ex vivo analysis was performed after 33 days

329 and demonstrated in 3 out of 6 animals a BLI signal emerging from the stroke region,

330 corroborating the in vivo measurements and excluding that the signal originated from the skin

331 (Fig. 2D). Although the BLI signal emerging from the stroke area could result from

332 accumulation of migrating SVZ progeny, alternatively, mature astrocytes in the infarction zone

333 might have dedifferentiated upon injury, resulting in nestin and subsequent Fluc activity (Buffo

334 et al., 2008). Thus, although a stroke-induced neurogenic response can be detected with *in vivo*

335 BLI in Nestin-CreERT2/Fluc mice, the exact origin of the BLI signal could

336 not be identified.

337

338 *Development and validation of conditional Cre-Flex LVs for specific eNSC labeling*

339

340 To overcome this limitation, we engineered a viral vector-based system, containing a Cre-Flex

341 cassette. The LV encodes a reporter cassette, here encoding eGFP and Fluc linked by a peptide

342 2A sequence, in reverse orientation relative to the promoter, that is only activated in cells

343 expressing Cre recombinase (LV-Cre-Flex Nb eGFP-T2A-Fluc; Fig. 3A). We injected LV-Cre-

344 Flex Nb eGFP-T2A-Fluc into Nestin-Cre transgenic mice, which express Cre recombinase under

345 the control of the rat nestin promoter and enhancer, limiting Cre expression to eNSCs. As a

346 result, eGFP and Fluc expression is specifically activated in eNSCs and their progeny. The use of

347 2A-like peptides results in equimolar expression of Fluc and eGFP reporter genes (Ibrahimi et

348 al., 2009), enabling BLI and immunohistochemistry for eGFP to identify transduced

349 cells in the same animal.

350

351

352
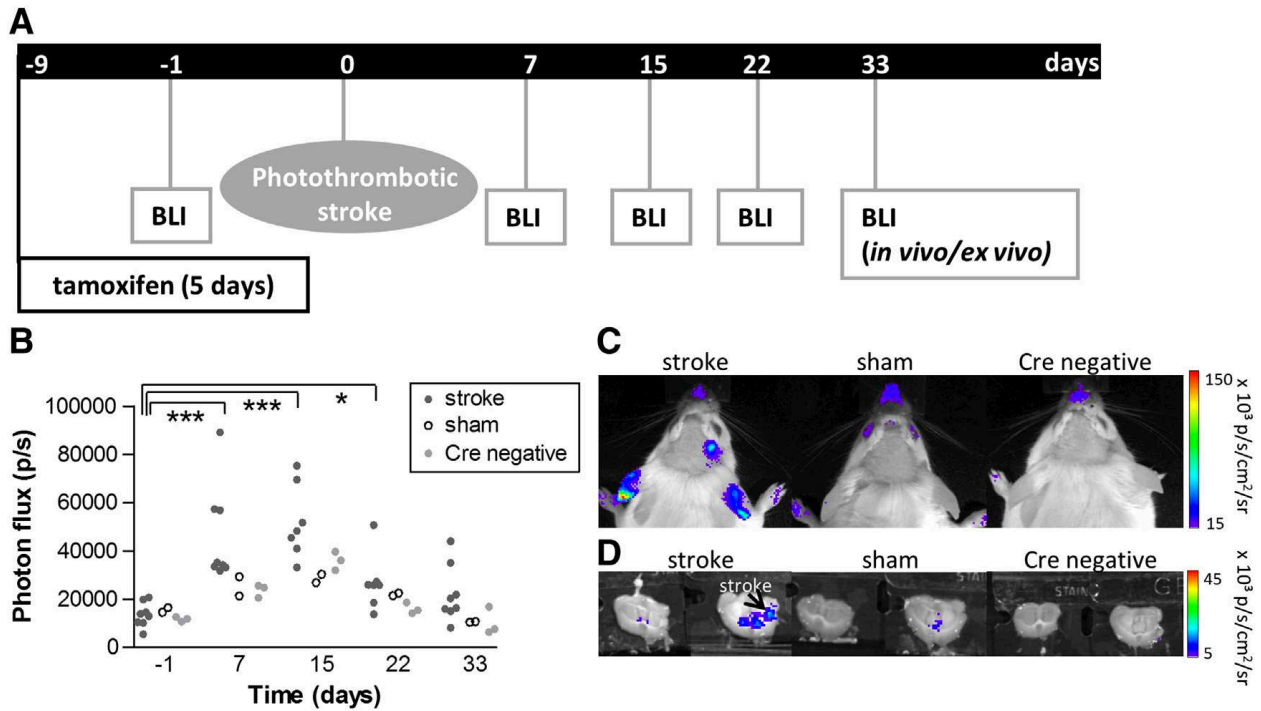
Fig. 2. Stroke induces an increase in BLI signal in Nestin-CreERT2/Fluc mice localized to the peri-infarct area. (A) Experimental time line for BLI measurements of Nestin-CreERT2/Fluc mice after a PT stroke. 9 days after the start of tamoxifen induction, mice received PT stroke (n=8) or sham (n= 2) surgery. Cre-negative littermates with stroke were included as controls (n =3). (B) Compared to the baseline scan performed before surgery, the in vivo BLI signal originating from the stroke region was 3.2±0.4 fold higher at 7 days (repeated measures one way ANOVA p b 0.001, followed by Dunnett's post test p b 0.001), 4.2 ± 0.5 fold higher at 15 days (Dunnett's post test p b 0.001), 2.1 ± 0.4 fold higher at 22 days (Dunnett's post test p b 0.05) and 1.9±0.3 fold higher at 33 days (not significant) in stroke animals. (C) Representative in vivo BLI signals 33 days after stroke. In 6 out of 8 Nestin-CreERT2/Fluc mice receiving stroke, a distinctive in vivo BLI signal originating from the stroke region could be detected, which could not be detected in sham or in Cre-negative animals. (D) Representative ex vivo BLI signals 33 days after stroke. In 3 of the 6 animals with an increased in vivo stroke BLI signal, an ex vivo BLI spot in the stroke region could be detected.

The LVs were injected in the SVZ of healthy adult Nestin-Cre mice (n = 9) to label the eNSCs

and the migration of the progeny to the OB was monitored by BLI at 1, 8, 15, 20 and 27 weeks

after injection (Figs. 3B,C). In line with earlier data (Reumers et al., 2008), a distinct BLI signal

emerged from the OB at 8 weeks, which gradually increased over time being 3.2 ± 0.3 fold

higher at 8 weeks (not significant), 4.3 ± 0.8 fold higher at 15 weeks (p b 0.01), 5.1 ± 1.1 fold

higher at 20 weeks (p b 0.001) and 5.5±1.4 fold higher at 27 weeks (p b 0.001) compared

to 1 week after injection (Figs. 3B,C). No BLI signal from the OB could be identified in WT

13

377 mice 1 or 15 weeks after injection of the Cre-Flex LV (n = 4) (Figs. 3B, C).

378 Immunohistochemical detection of Cre+ and eGFP+ cells showed specific labeling of cells lining

379 the ventricle wall and labeled eNSC progeny in the OB (Figs. 3D–E–F, respectively). In

380 conclusion, the conditional LV-based labeling system combines specific and efficient labeling of

381 the eNSC population of the SVZ with the possibility for immunohistochemical analysis of the

382 transduced eNSCs and their progeny. Additionally, migration of the eNSC progeny to the OB

383 could be monitored in vivo with BLI, which was not feasible in the Nestin-

384 CreERT2/Fluc mice.

385

386 *Stroke-induced neurogenic response in the SVZ is detected by BLI and histology*

387

388 Cre-Flex LVswere applied to monitor the eNSC response after stroke (Fig. 4A). Adult Nestin-

389 Cre mice were stereotactically injected with LVCre-Flex Nb eGFP-T2A-Fluc into the right side

390 of the SVZ. Seven days post injection, the animals received either a PT stroke in the right

391 sensorimotor cortex (n = 21) or sham surgery (n = 9). Stroke lesions were monitored with MRI 2,

392 7 and 14 days after surgery (Fig. 4C). BLI measurements were performed 1 day before (baseline)

393 and 2, 7, 14, 30 and 90 days after surgery (Figs. 4A,B,D). As a control, a Cre negative mouse

394 was injected with the LV-Cre-Flex vector and received a PT stroke. It was monitored until 3

395 months after stroke, but no BLI signal could be detected (data not shown). At all time points

396 investigated, the sham animals showed no difference in BLI signal compared to the baseline scan

397 (Fig. 4D). However, mice with a PT stroke showed a 4.3 ± 0.8 fold increase in BLI signal at 2

398 days (p b 0.001), a 6.2 ± 1.6 fold increase at 7 days (p b 0.01), a 7.5 ± 3.3 fold increase at 14

399 days (p b 0.05) and a 6.4 ± 3.5 fold increase at 30 days (not significant) (Fig. 4D). At later time

400 points, the stroke BLI signal decreased until 90 days after stroke.

401

402 The stroke-induced increase in BLI signal was corroborated by stereological quantification of the

403 number of eGFP+ cells in the SVZ, striatum, corpus callosum (CC) and peri-infarct area (Figs.

404 5A,B).Most eGFP+ cells were detected in the CC, reaching to the stroke area. In sham animals,

405 2116 ± 209 eGFP+ cells (n = 7) were counted and this number did not change over time. In

406 animals receiving stroke surgery, the number of eGFP+ cells was significantly higher at 2 days

407 $(4123 \pm 674$, p b 0.05, n = 7), 7 days $(5407 \pm 290$, p b 0.05, n = 2) and 14 days $(4610 \pm 222$, p b

408 0.05, n = 4) after stroke, compared to sham animals (Fig. 5B). 90 days after stroke, the number of

409 eGFP+ cells decreased and was significantly lower (2382 ± 375, p b 0.05, n = 7) compared to 7

410 and 14 days after stroke, corroborating the results obtained by BLI.

411
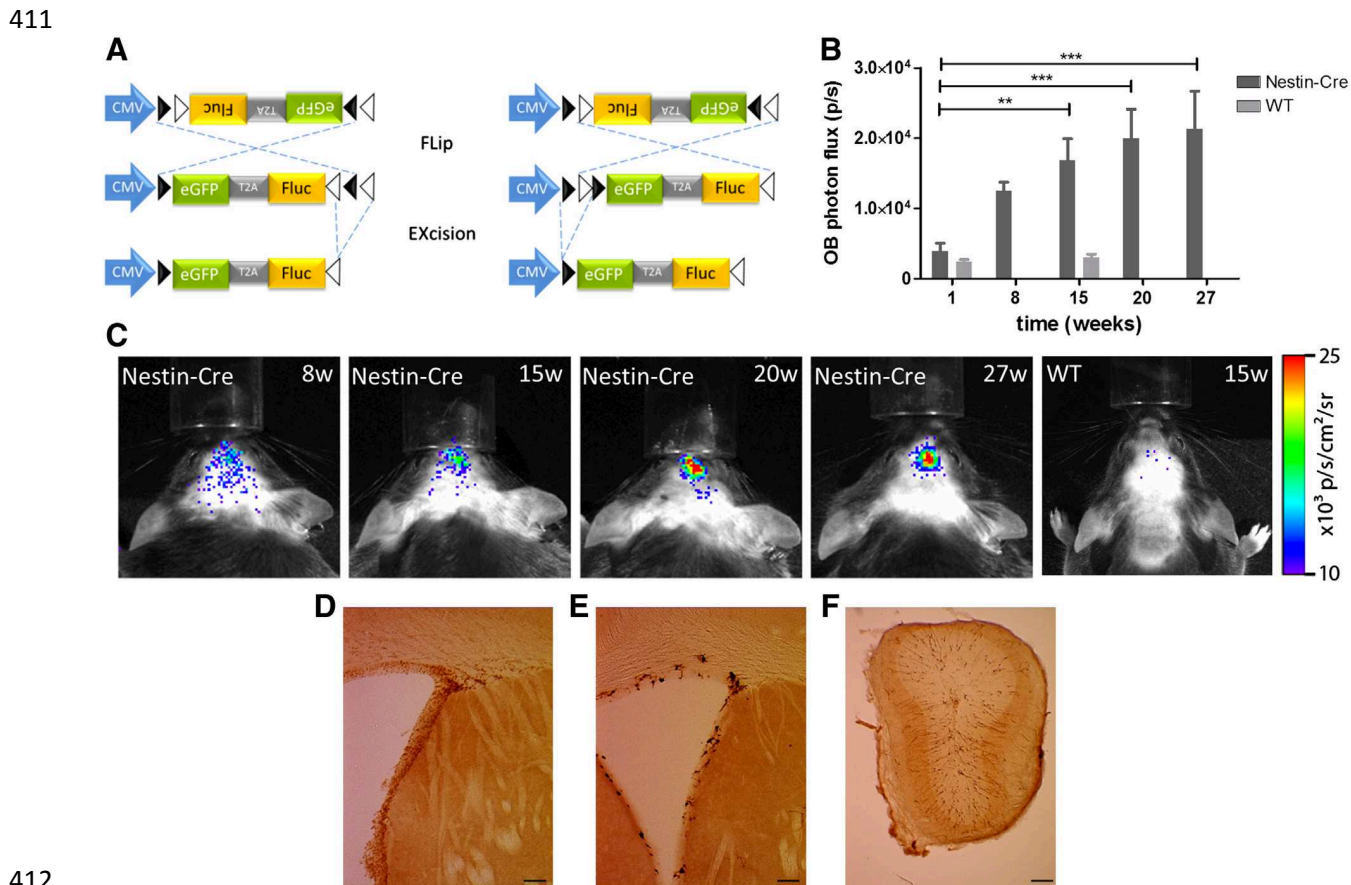
412
413 Fig. 3. Validation of conditional LV-Cre-Flex for specific eNSC labeling. (A) Schematic
414 representation of the conditional Cre-Flex LV. The cDNA cassette is flanked by one pair of loxP
415 sites (closed arrowheads) and one pair of loxm2 sites (open arrowheads). In the presence of Cre
416 recombinase, the DNA sequence between opposing sites is inversed (Flip), resulting in the
417 positioning of two homotypic sites in the same orientation. The DNA sequence that is flanked by
418 similarly oriented sites is excised (Excision). Cre-mediated inversion can start at the
419 loxP or the loxm2 sites, but will always result in the same final product after Cre-mediated
420 excision. The end product is an inverted DNA sequence, flanked by two heterotypic sites
421 that cannot recombine with one another thereby preventing further inversions. (B) Cre-Flex Nb
422 eGFP-T2A-Fluc LV were injected in the SVZ of black furred Nestin-Cre mice (n= 9) or
423 Cre-negative littermates (n= 4). The mice were scanned at 1, 8, 15, 20 and 27 weeks post
424 injection. A significant increase in BLI signal originating from the OB was detected over time
425 in the Nestin-Cre mice (repeated measures one-way ANOVA p = 0.001, followed by Dunnett's
426 post test). (C) Representative BLI images of Nestin-Cre and WT littermates at indicated
427 time points. Detection of Cre+ (D) and eGFP+ (E,F) cells in the SVZ and OB 4 weeks after
428 injection of Cre-Flex_Fluc Nb eGFP LV in the SVZ of Nestin-Cre mice (D–F) Scale bar= 250
429 μm.

430

To ensure that the eGFP+ cells originate from labeled eNSCs and not from reactive astrocytes that upregulate their nestin promoter and thus Cre upon injury, Cre expression was analyzed 2 days after stroke (Supplementary Figs. 3A,B). There was no Cre upregulation in the ipsilateral SVZ and CC compared to the contralateral hemisphere (Supplementary Fig. 3A), whereas Cre-positive cells with astrocyte-like morphology were detected in close proximity of the stroke lesion (Supplementary Fig. 3B). These cells were mainly present in the cortex on the dorsal side of the lesion and to a lesser extent on the lateral side of the lesion. Since the Cre-Flex LVs were injected in the SVZ, which is physically distant from the stroke region, and since the Cre-Flex LVs specifically label cells in the SVZ (Fig. 3E), it is unlikely that these distant reactive astrocytes were labeled directly via viral vector injection. Taken together the Cre-Flex LV allowed non-invasive monitoring of a stroke-induced transient increase in the number of eGFP+ cells, which originated from labeled eNSCs in the SVZ.

In vivo BLI reveals eNSCmigration to the area of infarction and OB following PT stroke

Long-term BLI follow-up of stroke animals not only revealed a transient increase in BLI signal, but also a clear shift of the BLI signal towards the stroke lesion was apparent (Fig. 4B). To estimate the migration of the BLI signal after stroke, the distance between the BLI hot spot and the midline was determined (Fig. 4E). Before stroke surgery, a unifocal signal originating from the site of injection was detected, which corresponds to labeled cells in the SVZ (average distance of 2.56 ± 0.22 mm from midline). Two days after stroke, a small shift of the BLI signal towards the contralateral hemisphere was evident (Fig. 4B), probably due to the induction of edema as was detected by MRI (Supplementary Fig. 4A). At 1 and 2 weeks after stroke, a significant shift of the BLI spot towards the stroke region was observed in 9 out of 10 animals (average distance of 4.62 ± 0.25 mm from midline, p b 0.001 compared to baseline) (Figs. 4B,E), suggesting migration of the eNSC progeny towards the stroke area. In the sham-operated animals no shift was detected at any of the time points (data not shown). Since dynamic changes of edema or changes in ventricle size due to loss of viable brain tissue might affect the location of the BLI signal, the animals were also imaged with MRI on the same day of the BLI (Fig. 4A). The needle tract was used as a reference and its shift due to edema formation or changes in ventricle size was monitored (Supplementary Figs. 4A,B). The needle tract shift 14 days after

stroke compared to the time of injection was 0.39±0.04mm(n=9),which was considerably smaller

than the shift of the BLI signal (2.06 mm). Although a small enlargement of the ventricles was

detected in the animals with a PT stroke, its effect on the migration of BLI signal was limited.
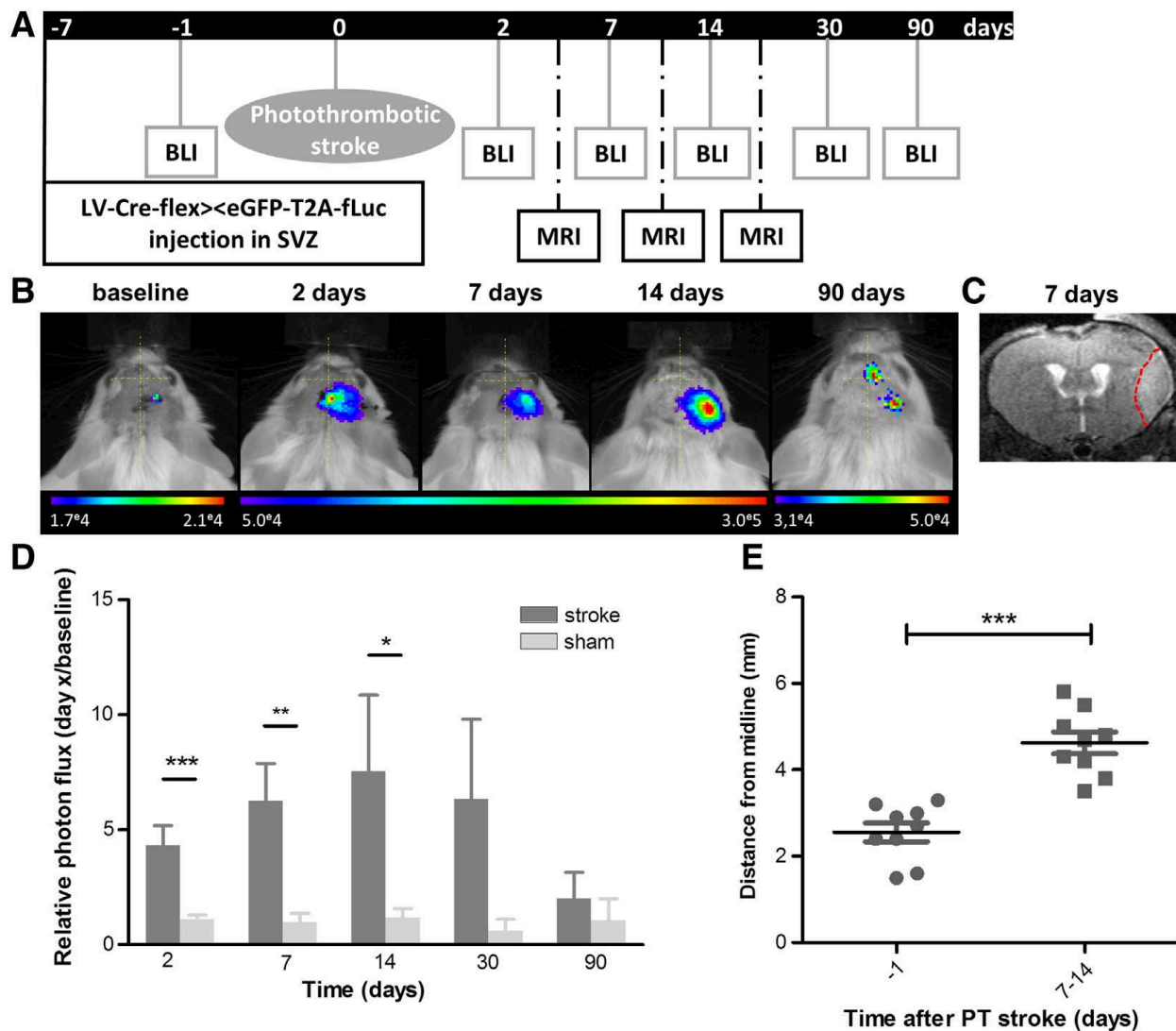
Fig. 4. BLI detects the increase and migration of eNSC progeny after PT stroke in Nestin-Cre
mice injected with the LV-Cre-Flex. (A) Experimental time line for imaging of the eNSC
response in a PT stroke model in mice. Seven days after stereotactic injection of LV-Cre-Flex in
the SVZ of Nestin-Cre mice, the animals received a PT stroke in the right sensorimotor cortex
(n=21) or sham surgery (n=9). The animals were imaged with BLI and MRI, for additional
anatomical information, at indicated time points. (B) Consecutive BLI images of a Nestin-Cre
mouse before and after stroke injury reveal a time-dependent increase of BLI signal and a shift of
the BLI signal towards the stroke lesion. Three months after stroke, a second BLI signal can be
discriminated between the eyes, representing migration of labeled eNSC progeny to the OB. This
signal could not be distinguished before and 2, 7, 14 days after stroke. (C) Representative T2-
weighted MR image 7 days after stroke surgery of a Nestin-Cre mouse. The stroke region in the

478 right sensory motor cortex is depicted with a red dotted line. (D) Quantification of relative BLI
479 signal. 2 days after stroke surgery, a 4.3 ± 0.8 fold increase in BLI signal emanating from the
480 SVZ was detected (n = 22) in comparison to the sham animals (n = 9) (Mann–Whitney test p b
481 0.001). A more pronounced increase (6.2 ± 1.6 fold) was detected at 7 days (n = 14 versus n = 9)
482 (p b 0.01), 14 days (7.5 ± 3.3 fold increase in stroke (n =8) versus sham (n=4) animals (p b 0.05))
483 and at 30days (6.4±3.5 fold increase in stroke (n=6) versus sham(n=2) animals) after surgery. 90
484 days after stroke surgery, a relative photon flux of 2.01 ±1.1 difference was detected in stroke
485 animals (n=7) compared to 1.1± 1.0 in sham animals (n=2). (E) Migration of the BLI hot spot
486 towards the stroke region. Before stroke surgery, the average distance of the BLI spot is 2.56 ±
487 0.22 mm from the midline (n = 9). 7–14 days after stroke surgery, the average distance of the
488 BLI spot is 4.62 ± 0.25 mm from the midline (n= 9, t-test p b 0.001).
489
490 Since most studies have investigated stroke-induced neurogenesis in models of middle cerebral

491 artery occlusion (MCAO) (Parent et al., 2002; Thored et al., 2007), a small experiment where

492 animals received either MCAO (n=4) or sham surgery (n=3) was performed (Supplementary

493 Fig. 5). The MCAO model provides MCA territory infarctions, involving the striatum and the

494 frontoparietal cortex, after the insertion of a monofilament that blocks the origin of MCA,

495 whereas the PT stroke model involves the intravenous administration of a photosensitive dye

496 followed by laser irradiation of any exposed region of the skull.

497

498 Although a 5 fold increase in BLI signal was detected over time in the animal with the largest

499 MCAO stroke lesion, there was no re-location of the BLI signal, most likely due to the large

500 stroke size and its location, which restrains the migration and localization of the labeled cells

501 within a region of the ischemic striatum (Ohab and Carmichael, 2008).

502

503 In the group receiving PT stroke, long-term BLI follow-up revealed a clear BLI signal between

504 the eyes in 5 out of 8 animals at 3 months after stroke, in line with migration of eNSC progeny to

505 the OB (Fig. 4B). The origin of BLI signal emerging from the OB was corroborated

506 histologically by a gradual increase in the number of eGFP+ cells in the OB over time, being 2.7

507 ± 0.6 fold higher at 14 days (not significant) and 12.8 ± 2.0 fold higher (p b 0.05) at 90 days

508 compared to 7 days after stroke surgery (Figs. 5C,D). These results provide additional evidence

509 that the LV-Cre-Flex specifically labeled the eNSCs in the SVZ.

510

511 In conclusion, injection of LV-Cre-Flex in the SVZ of Nestin-Cre mice allowed monitoring both

512 the migration of eNSC progeny from the SVZ

513   to the stroke region and to the OB with BLI.
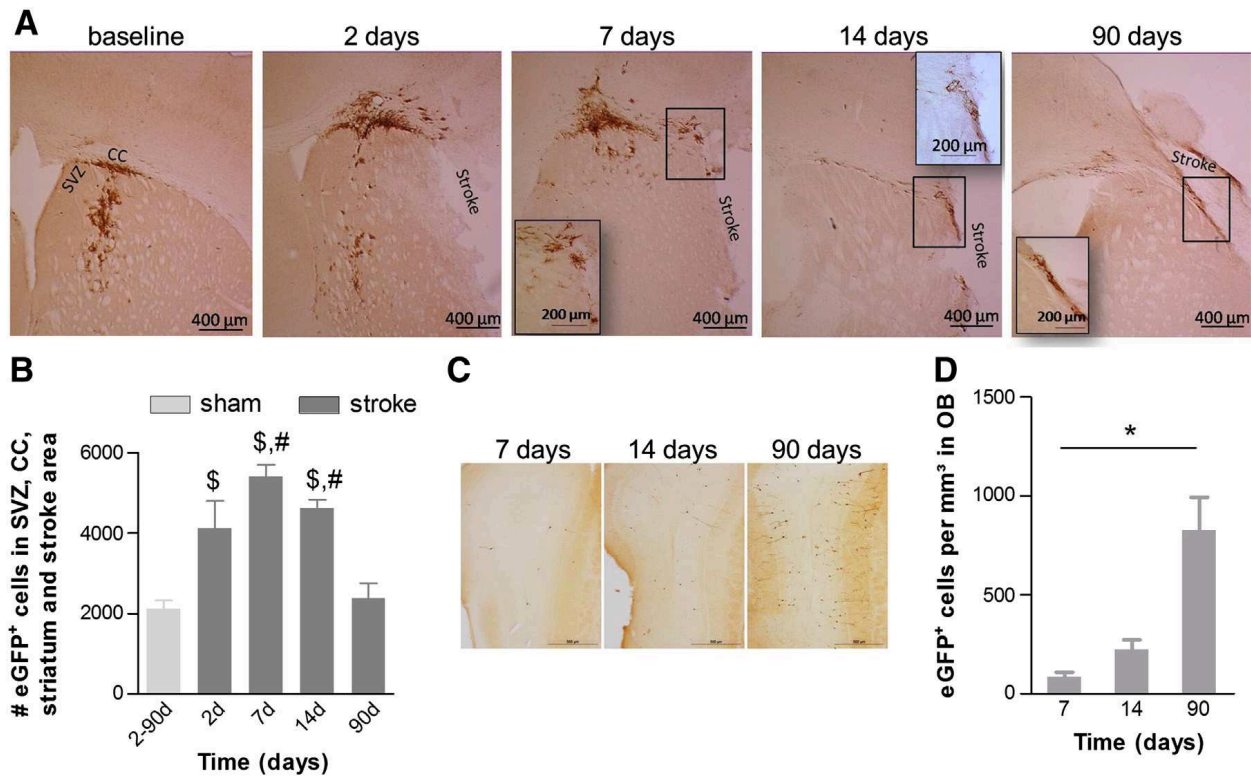
Fig. 5. Histological characterization of long-term stroke-induced eNSC response. (A)
Representative immunohistochemistry for eGFP of the SVZ, CC and stroke area at baseline and
2, 7, 14 days and 3 months after stroke surgery. Most eGFP+ cells were detected in the CC, with
some cells reaching the stroke area. The presence of eGFP+ cells surrounding the stroke area is
most pronounced at 14 days and 3 months after surgery. Magnifications of specific details are
integrated in the figure. (B) Stereological quantification of the total number of eGFP+ cells in the
SVZ, CC, striatum and stroke area after PT stroke. In sham animals, the number of eGFP+ cells
was constant over time and on average 2116 ± 210 eGFP+ cells were detected (n = 7). In stroke
animals, the number of eGFP+ cells was significantly higher at 2 days (4123 ± 674, n = 7), 7
days (5407 ± 290, n = 2) and 14 days (4610 ± 222, n = 4) after stroke, compared to sham animals
(One-way ANOVA p b 0.001, followed by Bonferroni post test p b 0.05, indicated by $). 90 days
after stroke, the number of eGFP+ cells was significantly lower (2382 ± 375, n=7, Bonferroni post
test p b 0.05, indicated by #) compared to 7 and 14 days after stroke. (C) Representative
immunohistochemical images of eGFP+ cells in the OB of mice with PT stroke at 7, 14 and 90
days after surgery. (D) Stereological quantification of the number of eGFP+ cells in the OB at 7
days (84 ± 24, n=2), 14 days (225 ± 48, n =4) and 90 days (825 ± 167, n=7) after stroke. 3 months
after stroke, the number of eGFP+cells was significantly higher compared to 7 days after stroke
(Kruskal-Wallis test p b 0.05, followed by Dunn's post test p b 0.05). The time-dependent
increase corresponds to the migration of eGFP+ eNSC progeny from the SVZ to the OB.
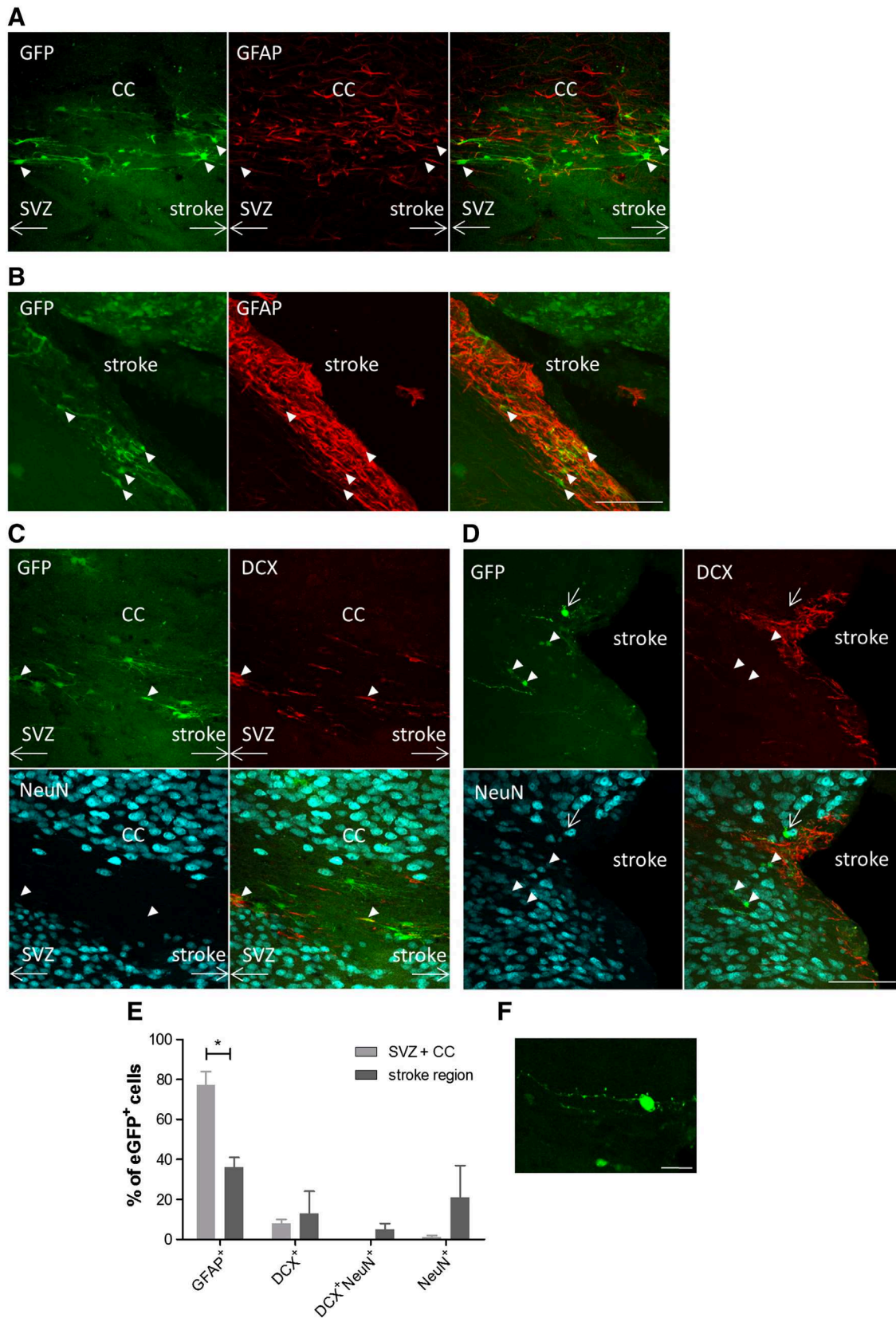
535
536 Fig. 6. Labeled eNSCs differentiate into astrocytes and neurons in the stroke region. (A,B)
537 Double immunofluorescence staining for eGFP (green) and GFAP (red) of the CC (A) and stroke

region (B) of the ipsilateral hemisphere 90 days after stroke. Filled white arrowheads indicate eGFP+ eNSCs and astrocytes. (C,D) Triple immunofluorescence staining for eGFP (green), DCX (red) and NeuN (blue) of the CC (C) and stroke region (D). (C) Filled white arrowheads indicate eGFP+ migrating neuroblasts. (D) Filled white arrowheads and arrow indicate eGFP+ mature neurons. (E) Quantification of double and triple labeled cells. (F) Magnification of eGFP+ neuron indicated with arrow in (D). Scale bar: (A–D)= 100 μm; (F) = 25 μm.

eNSC progeny differentiates into astrocytes and neurons in the peri-infarct region

Since injection of LV-Cre-Flex in Nestin-Cre mice results in the expression of Fluc and eGFP in the eNSCs and their progeny, a detailed histological analysis of the transduced cell population and its progeny can be performed. In animals killed 90 days after PT stroke, light producing cells (152 ± 30 eGFP+ cells counted per animal, n = 3) were identified by double and triple immunofluorescence stainings (eGFP in combination with GFAP or DCX and NeuN (Fig. 6)). In the SVZ and the CC, 77 ± 7% of eGFP+ cells were GFAP+ eNSCs and astrocytes, 8 ± 2% were DCX+ migrating neuroblasts and b1% were NeuN+ mature neurons (Figs. 6A,C,E). A different pattern of cellular phenotypes was detected in the peri-infarct region: 36 ± 5% of eGFP+ cells were GFAP+ astrocytes, 13 ± 11% were DCX+ migrating neuroblasts, 5 ± 3% were DCX+NeuN+ immature neurons and 21 ± 16% were NeuN+ mature neurons (Figs. 6B,D,E). Evaluation of differentiation into mature neurons, displayed a high inter-animal variability, with one animal showing 50% of eGFP+ cells co-expressing NeuN in the peri-infarct region, while the other two animals showed less than 10% coexpression. In the first animal, some eGFP+ neurons showed long dendrites covered with many spines (Fig. 6F). These data indicate that the labeled eNSCs in the SVZ gave rise to progeny that migrated towards the stroke region where they eventually differentiated into both astrocytes and mature neurons.

Discussion

Detailed knowledge of the biological role and potential of eNSCs is of great importance for the success of neuro-regenerative therapies in different neurological disorders, including stroke. Therefore, development of non-invasive methods to monitor and study proliferation, migration and survival of eNSCs and their progeny in the same animal over time is crucial. The main dvantage of cell tracking via BLI is the high sensitivity, especially when cells are located in superficial tissues (Massoud and Gambhir, 2003). The present study demonstrates non-invasive imaging of the eNSC response after PT stroke in a mouse model using BLI. First, we generated double transgenic Nestin-CreERT2/Fluc mice, in which Fluc expression is induced in the eNSCs after tamoxifen administration. After stroke, these mice showed an increase in BLI signal in vivo (n = 6/8) and ex vivo (n = 3/8) originating from the stroke lesion (Figs. 2B, C). The discrepancy in efficiency between the in vivo and ex vivo results can be explained by technical issues, such as the time required to dissect the brain tissue immediately after sacrifice, which causes differences in oxygenation status of the tissue and enzymatic activity (Deroose et al., 2006). In the latter model it was impossible to define the origin of the cells giving rise to the BLI signal emerging from the stroke area, which might either originate from accumulation of migrating SVZ progeny or from dedifferentiation of local mature astrocytes upon injury, resulting in nestin and subsequently, Fluc expression (Buffo et al., 2008). Moreover, although Fluc is expressed in eNSCs of the SVZ and eventually in the progeny arriving in the OB, as was evidenced by ex vivo BLI (Figs. 1D, E), the number of labeled cells or the expression level of Fluc per cell was too low for in vivo detection (Figs. 1A–C). In this way, the effect of stroke on the neurogenic process towards the OB could also not be monitored.

In a second approach, we circumvented these drawbacks by devising conditional Cre-Flex LVs to inject in the SVZ of Nestin-Cre mice. Specific induction of Fluc and eGFP in the eNSCs and their progeny allows both BLI and immunohistochemical characterization of the neurogenic process. In contrast to the first approach using double transgenic mice, in vivo BLI signals from the SVZ and eventually from the OB could be detected (Fig. 3C),most probably due to the higher Fluc expression levels. Induction of a PT stroke resulted in a significant gradual increase in BLI signal between 2 days and 2 weeks after surgery (Figs. 4B,D). The latter was underscored by an increase in eGFP+ cells in the SVZ, striatum, CC and stroke region (Fig. 5B). Subsequently, the

22

594   BLI signal and the number of eGFP+ cells decreased to background levels at 3 months after

595   stroke. This transient increase in eNSC progeny is in accordance with two studies describing a

596   transient increase in the proliferation and migration of eNSCs following stroke or brain trauma,

597   detected by histology using cell type-specific markers (Parent et al., 2002) or by retroviral

598   labeling of SVZ cells (Goings et al., 2004). Parent et al. showed that the number of BrdU-labeled

599   cells was lower 5 weeks after stroke compared to previous time points, suggesting that many of

600   the newly generated cells died (Parent et al., 2002).

601

602   In Nestin-Cre mice injected with the Cre-Flex LV, a clear relocalization of the BLI signal

603   towards the stroke area was detected between 1 and 2 weeks after stroke surgery. This was

604   confirmed histologically by eGFP+ cells moving closer towards the ischemic lesion over

605   time (Figs. 4B and 5A). The 1–2 weeks time frame of this migration is in agreement with the

606   work of Ohab et al. who detected GFP+ cells, originating from the SVZ, in the peri-infarct cortex

607   7 and 14 days after stroke (Ohab et al., 2006). When monitoring eNSC migration after stroke

608   with BLI, we encountered some technical hurdles. First, edema formation causes a shift of the

609   midline, resulting in a slight apparent re-location of the BLI spot towards the contralateral

610   hemisphere, complicating detection of eNSC migration towards the lesion at early time points.

611   Second, changes in ventricle size, due to tissue degeneration after stroke may confound the

612   imaging results (Karki et al., 2010). Therefore, we combined BLI with MRI, which has a high

613   spatial resolution and gives better insight in alterations of the anatomical structure of the brain.

614

615   Since labeled cells express a fluorescent reporter (eGFP) in addition to the bioluminescent Fluc

616   reporter, the origin and identity of light emitting cells could be determined by

617   immunohistochemical stainings. Ninety days after stroke, labeled eNSC progeny differentiated

618   into both astrocytes and mature neurons, demonstrating the multipotency of eNSCs upon stroke

619   injury (Arvidsson et al., 2002; Goings et al., 2004; Parent et al., 2002). The majority of eGFP+

620   labeled cells in the SVZ, CC and the stroke region expressed GFAP, corroborating astrocytic

621   differentiation of eNSC progeny after cortical injury (Goings et al., 2004; Holmin et al., 1997).

622   In addition, using tamoxifen-inducible Nestin-CreERT2:R26R-YFP reporter mice, Li et al.

623   demonstrated that 45% of eNSC progeny co-expressed GFAP 6 weeks after MCAO, indicating a

624   significant gliogenic component (Li et al., 2010).

625

Since stroke injury might induce nestin expression in reactive astrocytes (Buffo et al., 2008; Shimada et al., 2010; Sirko et al., 2013) or in vasculature-associated cells in the ischemic core (Shin et al., 2013), one could question the source of the eGFP+ cells located around the ischemic lesion. However, it has been well described that reactive astrocytes are mainly present in the close vicinity of the stroke region. Unbiased stereological quantifications of astrocyte proliferation, a hallmark of reactive gliosis, showed that astrocytes respond to stroke injury in a spatially graded way (Barreto et al., 2011). The authors showed that most astrocyte proliferation occurs within 200 μm of the edge of the infarct. In addition, nestin upregulation of reactive astrocytes has been shown to be confined to the peri-infarct region, or to clearly demarcate the lesion boundary (Li and Chopp, 1999; Shimada et al., 2010). Since we injected the Cre-Flex LV in the SVZ, which is physically distant from the stroke region, and since we did not detect any changes in Cre expression in the SVZ or CC, we consider it unlikely to label local reactive astrocytes around the stroke region. Another indication that argues against local reactive astrocytes as the main origin of labeled cells concerns the localization of the BLI signal: if the 4.3 fold increase in BLI signal two days after stroke would be caused by labeling of reactive astrocytes, one would expect appearance of a new BLI spot emerging from the stroke region, or a shift of the existing SVZ BLI spot towards the stroke region. However, we show that this is not the case and that there is even a small shift of the original SVZ BLI spot towards the contralateral side (Fig. 4B). A clear migration of the BLI spot towards the stroke region was only apparent after 7–14 days after stroke. Our data strongly suggest migration of the progeny of transduced eNSCs via the CC to the stroke lesion. The increase in BLI signal between the eyes and the corresponding increase in the number of eGFP+ cells in the OB over time, points to the migration of labeled eNSC progeny from the SVZ to the OB, proving that the eNSCs in the SVZ were labeled by the Cre-Flex LV. Several research groups have shown a reduction or diversion of normal neuroblast migration from the SVZ to the OB at early time points after cortical lesion or stroke (Goings et al., 2004; Ohab et al., 2006). The Cre-Flex LV technology will allow longitudinal non-invasive imaging of the effects of brain lesions on rostral migration.

The present study focuses on the response of SVZ-derived Nestin+ eNSCs on stroke injury. However, none of the eNSC markers currently available exclusively labels eNSCs and evidence

656 emerges suggesting eNSC heterogeneity both in the SVZ (Giachino et al., 2013) and the

657 SGZ (Bonaguidi et al., 2012; DeCarolis et al., 2013). It would therefore be interesting to apply

658 the Cre-Flex LVs in different transgenic mice to compare the contribution of different progenitor

659 populations to the stroke-induced neurogenic response (Dhaliwal and Lagace, 2011). In addition,

660 the Cre-Flex LVs might also be used to study eNSC response in other disease models

661 (Guglielmetti et al., 2013).

662

663 In conclusion, we developed a novel technique based on conditional Cre-Flex LVs that allows

664 non-invasive imaging of the stroke-induced eNSC response in living mice with BLI. In addition,

665 this new technique enables fate mapping of the eNSC progeny after stroke by

666 immunohistochemistry. Our BLI and histological data are consistent with the prevailing

667 hypothesis that stroke induces a transient increase in proliferation in the SVZ, a targeted

668 migration of eNSC progeny towards the stroke region and differentiation in both astrocytes and

669 neurons. For this reason, we believe that this technology may facilitate preclinical validation of

670 neuro-regenerative strategies in rodent stroke models.

671

672 Supplementary data to this article can be found online at

673 http://dx.doi.org/10.1016/j.nbd.2014.05.014.

674

675 **Conflict of interest statement**

676 The authors declare that they have no conflict of interest.

677

692
693

References

Altman, J., 1962. Are new neurons formed in the brains of adult mammals? Science 135, 1127–1128.

Altman, J., 1963. Autoradiographic investigation of cell proliferation in the brains of rats and cats. Anat. Rec. 145, 573–591.

Alvarez-Buylla, A., Garcia-Verdugo, J.M., 2002. Neurogenesis in adult subventricular zone. J. Neurosci. 22, 629–634.

Arvidsson, A., Collin, T., Kirik, D., Kokaia, Z., Lindvall, O., 2002. Neuronal replacement from endogenous precursors in the adult brain after stroke. Nat. Med. 8, 963–970. http://dx.doi.org/10.1038/nm747.

Baekelandt, V., Claeys, A., Eggermont, K., Lauwers, E.,De Strooper, B.,Nuttin, B.,Debyser, Z., 2002. Characterization of lentiviral vector-mediated gene transfer in adult mouse brain. Hum. Gene Ther. 13, 841–853. http://dx.doi.org/10.1089/10430340252899019.

Baekelandt, V., Eggermont, K., Michiels, M., Nuttin, B., Debyser, Z., 2003. Optimized lentiviral vector production and purification procedure prevents immune response after transduction of mouse brain. Gene Ther. 10, 1933–1940. http://dx.doi.org/10.1038/sj.gt.3302094.

Barreto, G.E., Sun, X., Xu, L., Giffard, R.G., 2011. Astrocyte proliferation following stroke in the mouse depends on distance from the infarct. PLoS ONE 6, e27881. http://dx.doi.org/10.1371/journal.pone.0027881.

Bonaguidi, M.A., Song, J., Ming, G., Song, H., 2012. A unifying hypothesis on mammalian neural stem cell properties in the adult hippocampus. Curr. Opin. Neurobiol. 22, 754–761. http://dx.doi.org/10.1016/j.conb.2012.03.013.

Buffo, A., Rite, I., Tripathi, P., Lepier, A., Colak, D., Horn, A.-P.,Mori, T., Götz, M., 2008. Origin and progeny of reactive gliosis: a source of multipotent cells in the injured brain. Proc. Natl. Acad. Sci. U. S. A. 105, 3581–3586. http://dx.doi.org/10.1073/pnas.0709002105.

Collin, T., Arvidsson, A., Kokaia, Z., Lindvall, O., 2005. Quantitative analysis of the generation of different striatal neuronal subtypes in the adult brain following excitotoxic injury. Exp. Neurol. 195, 71–80. http://dx.doi.org/10.1016/j.expneurol.2005.03.017.

Couillard-Despres, S., Finkl, R.,Winner, B., Ploetz, S.,Wiedermann, D., Aigner, R., Bogdahn, U., Winkler, J., Hoehn, M., Aigner, L., 2008. In vivo optical imaging of neurogenesis: watching new neurons in the intact brain. Mol. Imaging 7, 28–34. http://dx.doi.org/10.2310/7290.2008.0004.

Curtis, M.A., Penney, E.B., Pearson, J., Dragunow, M., Connor, B., Faull, R.L.M., 2005. The distribution of progenitor cells in the subependymal layer of the lateral ventricle in the normal

and Huntington's disease human brain. Neuroscience 132, 777–788.
http://dx.doi.org/10.1016/j.neuroscience.2004.12.051.

DeCarolis, N.A., Mechanic, M., Petrik, D., Carlton, A., Ables, J.L., Malhotra, S., Bachoo, R.,
Götz, M., Lagace, D.C., Eisch, A.J., 2013. In vivo contribution of nestin- and GLAST-lineage
cells to adult hippocampal neurogenesis. Hippocampus 23, 708–719.
http://dx.doi.org/10.1002/hipo.22130.

Deierborg, T., Staflin, K., Pesic, J., Roybon, L., Brundin, P., Lundberg, C., 2009. Absence of
striatal newborn neurons with mature phenotype following defined striatal and cortical
excitotoxic brain injuries. Exp. Neurol. 219, 363–367. http://dx.doi.org/10.1016/j.
expneurol.2009.05.002.

Deroose, C.M., Reumers, V., Gijsbers, R., Bormans, G., Debyser, Z., Mortelmans, L.,
Baekelandt, V., 2006. Noninvasive monitoring of long-term lentiviral vector mediated
gene expression in rodent brain with bioluminescence imaging. Mol. Ther. 14, 423–431.
http://dx.doi.org/10.1016/j.ymthe.2006.05.007.

Dhaliwal, J., Lagace, D.C., 2011. Visualization and genetic manipulation of adult neurogenesis
using transgenic mice. Eur. J. Neurosci. 33, 1025–1036. http://dx.doi.org/10.1111/j.1460-
9568.2011.07600.x.

Dirnagl, U., members of the MCAO-SOP group, 2009. Standard operating procedures (SOP) in
experimental stroke research: SOP for middle cerebral artery occlusion in the mouse. Nature
Precedings. http://dx.doi.org/10.1038/npre.2009.3492.1.

Eriksson, P.S., Perfilieva, E., Björk-Eriksson, T., Alborn, A.M., Nordborg, C., Peterson, D.A.,
Gage, F.H., 1998. Neurogenesis in the adult human hippocampus. Nat. Med. 4, 1313–1317.
http://dx.doi.org/10.1038/3305.

Flynn, R.W.V., MacWalter, R.S.M., Doney, A.S.F., 2008. The cost of cerebral ischaemia.
Neuropharmacology 55, 250–256. http://dx.doi.org/10.1016/j.neuropharm.2008.05.031.

Geraerts, M., Michiels, M., Baekelandt, V., Debyser, Z., Gijsbers, R., 2005. Upscaling of
lentiviral vector production by tangential flow filtration. J. Gene Med. 7, 1299–1310.
http://dx.doi.org/10.1002/jgm.778.

Geraerts, M., Eggermont, K., Hernandez-Acosta, P., Garcia-Verdugo, J.-M., Baekelandt, V.,
Debyser, Z., 2006. Lentiviral vectors mediate efficient and stable gene transfer in adult neural
stem cells in vivo. Hum. Gene Ther. 17, 635–650. http://dx.doi.org/10.1089/hum.2006.17.635.

Giachino, C., Basak, O., Lugert, S., Knuckles, P., Obernier, K., Fiorelli, R., Frank, S., Raineteau,
O., Alvarez-Buylla, A., Taylor, V., 2013. Molecular diversity subdivides the adult forebrain
neural stem cell population. Stem Cells. http://dx.doi.org/10.1002/stem.1520.

Goings, G.E., Sahni, V., Szele, F.G., 2004. Migration patterns of subventricular zone cells in

786 adultmice change after cerebral cortex injury. Brain Res. 996, 213–226.
787 http://dx.doi.org/10.1002/jnr.22109.

789 Gray, W.P., Sundstrom, L.E., 1998. Kainic acid increases the proliferation of granule cell
790 progenitors in the dentate gyrus of the adult rat. Brain Res. 790, 52–59.
791 http://dx.doi.org/10.1016/S0006-8993(98)00030-4.

793 Guglielmetti, C., Praet, J., Rangarajan, J.R., Vreys, R., De Vocht, N., Maes, F., Verhoye, M.,
794 Ponsaerts, P., Van der Linden, A., 2013. Multimodal imaging of subventricular zone neural
795 stem/progenitor cells in the cuprizone mouse model reveals increased neurogenic potential for
796 the olfactory bulb pathway, but no contribution to remyelination of the corpus callosum.
797 NeuroImage. http://dx.doi.org/10.1016/j.neuroimage.2013.07.080 (Epub ahead of print).

799 Holmin, S., Almqvist, P., Lendahl, U., Mathiesen, T., 1997. Adult nestin-expressing
800 subependymal cells differentiate to astrocytes in response to brain injury. Eur. J.
801 Neurosci. 9, 65–75.

803 Ibrahimi, A., Vande Velde, G., Reumers, V., Toelen, J., Thiry, I., Vandeputte, C., Vets, S.,
804 Deroose, C., Bormans, G., Baekelandt, V., Debyser, Z., Gijsbers, R., 2009. Highly efficient
805 multicistronic lentiviral vectors with peptide 2A sequences. Hum. Gene Ther. 20, 845–860.
806 http://dx.doi.org/10.1089/hum.2008.188.

808 Jin, K., Minami, M., Lan, J.Q., Mao, X.O., Batteur, S., Simon, R.P., Greenberg, D.A., 2001.
809 Neurogenesis in dentate subgranular zone and rostral subventricular zone after focal cerebral
810 ischemia in the rat. Proc. Natl. Acad. Sci. U. S. A. 98, 4710–4715.
811 http://dx.doi.org/10.1073/pnas.081011098.

813 Karki, K., Knight, R.A., Shen, L.H., Kapke, A., Lu, M., Li, Y., Chopp, M., 2010. Chronic brain
814 tissue remodeling after stroke in rat: a 1-year multiparametric magnetic resonance imaging study.
815 Brain Res. 1360, 168–176. http://dx.doi.org/10.1016/j.brainres.2010.08.098.

817 Kempermann, G., Kuhn, H.G., Gage, F.H., 1997. Genetic influence on neurogenesis in the
818 dentate gyrus of adult mice. Proc. Natl. Acad. Sci. U. S. A. 94, 10409–10414.

820 Kernie, S.G., Parent, J.M., 2010. Forebrain neurogenesis after focal Ischemic and traumatic
821 brain injury. Neurobiol. Dis. 37, 267–274. http://dx.doi.org/10.1016/j.nbd.2009.11.002.

823 Komitova, M., Perfilieva, E.,Mattsson, B., Eriksson, P.S., Johansson, B.B., 2006. Enriched
824 environment after focal cortical ischemia enhances the generation of astroglia and NG2
825 positive polydendrocytes in adult rat neocortex. Exp. Neurol. 199, 113–121.
826 http://dx.doi.org/10.1016/j.expneurol.2005.12.007.

828 Lagace, D.C., Whitman, M.C., Noonan, M.A., Ables, J.L., DeCarolis, N.A., Arguello, A.A.,
829 Donovan, M.H., Fischer, S.J., Farnbauch, L.A., Beech, R.D., DiLeone, R.J., Greer, C.A.,
830 Mandyam, C.D., Eisch, A.J., 2007. Dynamic contribution of nestin-expressing stem cells to adult
831 neurogenesis. J. Neurosci. 27, 12623–12629. http://dx.doi.org/10.1523/JNEUROSCI.3812-

07.2007.

Lemberger, T., Parlato, R., Dassesse, D., Westphal,M., Casanova, E., Turiault,M., Tronche, F., Schiffmann, S.N., Schütz, G., 2007. Expression of Cre recombinase in dopaminoceptive neurons. BMC Neurosci. 8, 4. http://dx.doi.org/10.1186/1471-2202-8-4.

Li, Y., Chopp, M., 1999. Temporal profile of nestin expression after focal cerebral ischemia in adult rat. Brain Res. 838, 1–10. http://dx.doi.org/10.1016/S0006-8993(99)01502-4.

Li, L., Harms, K.M., Ventura, P.B., Lagace, D.C., Eisch, A.J., Cunningham, L.A., 2010. Focal cerebral ischemia induces a multi lineage cytogenic response from adult subventricular zone that is predominantly gliogenic. Glia 58, 1610–1619. http://dx.doi.org/10.1002/glia.21033.

Liu, J., Solway, K., Messing, R.O., Sharp, F.R., 1998. Increased neurogenesis in the dentate gyrus after transient global ischemia in gerbils. J. Neurosci. 18, 7768–7778.

Liu, F., You, Y., Li, X., Ma, T., Nie, Y., Wei, B., Li, T., Lin, H., Yang, Z., 2009. Brain injury does not alter the intrinsic differentiation potential of adult neuroblasts. J. Neurosci. 29, 5075–5087. http://dx.doi.org/10.1523/JNEUROSCI.0201-09.2009.

Massoud, T.F., Gambhir, S.S., 2003. Molecular imaging in living subjects: seeing fundamental biological processes in a new light. Genes Dev. 17, 545–580. http://dx.doi.org/10.1101/gad.1047403.

Ming, G., Song, H., 2005. Adult neurogenesis in the mammalian central nervous system. Annu. Rev. Neurosci. 28, 223–250. http://dx.doi.org/10.1146/annurev.neuro.28.051804.101459.

Nieman, B.J., Shyu, J.Y., Rodriguez, J.J., Garcia, A.D., Joyner, A.L., Turnbull, D.H., 2010. In vivo MRI of neural cell migration dynamics in the mouse brain. NeuroImage 50, 456–464. http://dx.doi.org/10.1016/j.neuroimage.2009.12.107.

Ohab, J.J., Carmichael, S.T., 2008. Poststroke neurogenesis: emerging principles of migration and localization of immature neurons. Neuroscientist 14, 369–380. http://dx.doi.org/10.1177/1073858407309545.

Ohab, J.J., Fleming, S., Blesch, A., Carmichael, S.T., 2006. A neurovascular niche for neurogenesis after stroke. J. Neurosci. 26, 13007–13016. http://dx.doi.org/10.1523/JNEUROSCI.4323-06.2006.

Oosterlinck, W.W., Dresselaers, T., Geldhof, V., Van Santvoort, A., Robberecht, W., Herijgers, P., Himmelreich, U., 2011. Response of mouse brain perfusion to hypo and hyperventilation measured by arterial spin labeling. Magn. Reson. Med. 66, 802–811. http://dx.doi.org/10.1002/mrm.23060.

Parent, J.M., Vexler, Z.S., Gong, C., Derugin, N., Ferriero, D.M., 2002. Rat forebrain neurogenesis and striatal neuron replacement after focal stroke. Ann. Neurol. 52, 802–813.

878 http://dx.doi.org/10.1002/ana.10393.

880 Reumers, V., Deroose, C.M., Krylyshkina, O., Nuyts, J., Geraerts, M., Mortelmans, L., Gijsbers,
881 R., Van den Haute, C., Debyser, Z., Baekelandt, V., 2008. Noninvasive and quantitative
882 monitoring of adult neuronal stem cell migration in mouse brain using bioluminescence imaging.
883 Stem Cells 26, 2382–2390. http://dx.doi.org/10.1634/stemcells.2007-1062.

885 Rueger, M.A., Backes, H., Walberer, M., Neumaier, B., Ullrich, R., Simard, M.-L., Emig, B.,
886 Fink, G.R., Hoehn, M., Graf, R., Schroeter, M., 2010. Noninvasive imaging of endogenous
887 neural stem cell mobilization in vivo using positron emission tomography. J.
888 Neurosci. 30, 6454–6460. http://dx.doi.org/10.1523/JNEUROSCI.6092-09.2010.

890 Safran,M., Kim,W.Y., Kung, A.L., Horner, J.W., DePinho, R.A., Kaelin Jr., W.G., 2003. Mouse
891 reporter strain for noninvasive bioluminescent imaging of cells that have undergone Cre-
892 mediated recombination. Mol. Imaging 2, 297–302.

894 Shapiro, E.M., Gonzalez-Perez, O., Manuel García-Verdugo, J., Alvarez-Buylla, A., Koretsky,
895 A.P., 2006.Magnetic resonance imaging of themigration of neuronal precursors generated in the
896 adult rodent brain. Neuroimage 32, 1150–1157.
897 http://dx.doi.org/10.1016/j.neuroimage.2006.04.219.

899 Shimada, I.S., Peterson, B.M., Spees, J.L., 2010. Isolation of locally derived stem/progenitor
900 cells fromthe peri-infarct area that do notmigrate fromthe lateral ventricle after cortical stroke.
901 Stroke 41, e552–e560. http://dx.doi.org/10.1161/STROKEAHA.110.589010.

903 Shin, Y.-J., Kim, H.L., Park, J.-M., Cho, J.M., Kim, S.Y., Lee, M.-Y., 2013. Characterization of
904 nestin expression and vessel association in the ischemic core following focal cerebral ischemia in
905 rats. Cell Tissue Res. 351, 383–395. http://dx.doi.org/10.1007/s00441-012-1538-x.

907 Sirko, S., Behrendt, G., Johansson, P.A., Tripathi, P., Costa,M.R., Bek, S., Heinrich, C., Tiedt,
908 S., Colak, D., Dichgans,M., Fischer, I.R., Plesnila, N., Staufenbiel,M., Haass, C., Snapyan,M.,
909 Saghatelyan, A., Tsai, L.-H., Fischer, A., Grobe, K., Dimou, L., Götz, M., 2013. Reactive glia in
910 the injured brain acquire stem cell properties in response to sonic hedgehog. Cell Stem Cell 12,
911 426–439. http://dx.doi.org/10.1016/j.stem.2013.01.019.

913 Sumner, J.P., Shapiro, E.M., Maric, D., Conroy, R., Koretsky, A.P., 2009. In vivo labeling of
914 adult neural progenitors for MRI with micron sized particles of iron oxide: quantification of
915 labeled cell phenotype. Neuroimage 44, 671–678.
916 http://dx.doi.org/10.1016/j.neuroimage.2008.07.050.

918 Thored, P., Wood, J., Arvidsson, A., Cammenga, J., Kokaia, Z., Lindvall, O., 2007. Long-term
919 neuroblast migration along blood vessels in an area with transient angiogenesis and increased
920 vascularization after stroke. Stroke 38, 3032–3039.
921 http://dx.doi.org/10.1161/STROKEAHA.107.488445.

923 Tronche, F., Kellendonk, C., Kretz, O., Gass, P., Anlag, K., Orban, P.C., Bock, R., Klein, R.,

924 Schütz, G., 1999. Disruption of the glucocorticoid receptor gene in the nervous system results in
925 reduced anxiety. Nat. Genet. 23, 99–103. http://dx.doi.org/10.1038/12703.
926
927 Vande Velde, G., Raman Rangarajan, J., Vreys, R., Guglielmetti, C., Dresselaers, T., Verhoye,
928 M., Van der Linden, A., Debyser, Z., Baekelandt, V., Maes, F., Himmelreich, U., 2012.
929 Quantitative evaluation of MRI-based tracking of ferritin-labeled endogenous neural
930 stem cell progeny in rodent brain. NeuroImage 62, 367–380.
931 http://dx.doi.org/10.1016/j.neuroimage.2012.04.040.
932
933 Vandeputte, C., Thomas, D., Dresselaers, T., Crabbe, A., Verfaillie, C., Baekelandt, V., Van
934 Laere, K., Himmelreich, U., 2011. Characterization of the inflammatory response in a
935 photothrombotic stroke model by MRI: implications for stem cell transplantation. Mol. Imaging
936 Biol. 13, 663–671. http://dx.doi.org/10.1007/s11307-010-0395-9.
937
938 Vreys, R., Vande Velde, G., Krylychkina, O., Vellema, M., Verhoye, M., Timmermans, J.-P.,
939 Baekelandt, V., Van der Linden, A., 2010. MRI visualization of endogenous neural progenitor
940 cell migration along the RMS in the adult mouse brain: validation of various MPIO labeling
941 strategies. Neuroimage 49, 2094–2103. http://dx.doi.org/10.1016/j.neuroimage.2009.10.034.
942
943 Watson, B.D., Dietrich, W.D., Busto, R., Wachtel, M.S., Ginsberg, M.D., 1985. Induction of
944 reproducible brain infarction by photochemically initiated thrombosis. Ann. Neurol. 17, 497–
945 504. http://dx.doi.org/10.1002/ana.410170513.
946
947 Zhang, R.L., Zhang, Z.G., Chopp, M., 2008. Ischemic stroke and neurogenesis in the
948 subventricular zone. Neuropharmacology 55, 345–352.
949 http://dx.doi.org/10.1016/j.neuropharm.2008.05.027.

Supplementary Figures
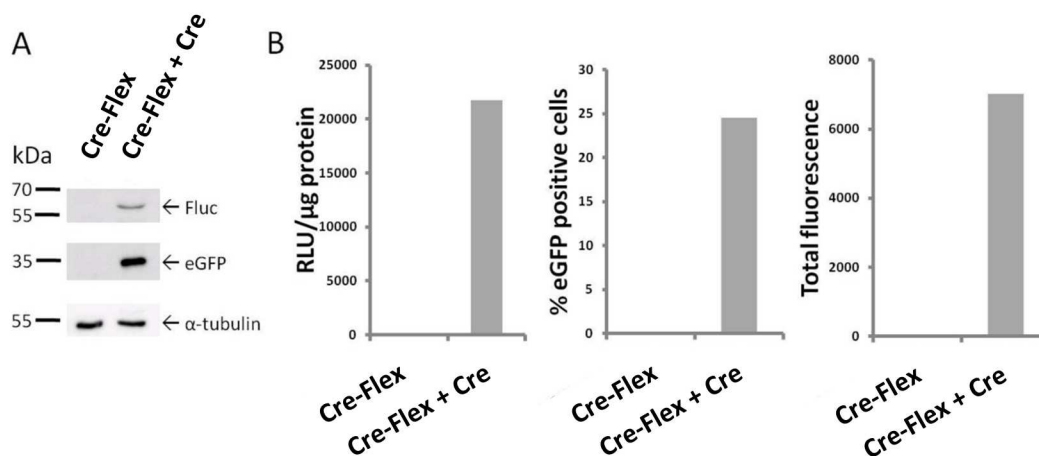
S Fig1. Validation of Cre-Flex LV in cell culture. (A) Western blot shows no detectable expression of eGFP or Fluc in 293T cells after transduction with Cre-Flex >< eGFP-T2A-Fluc LV; expression is induced when the cells are co-transduced with a LV encoding for Cre. (B) Luciferase activity and eGFP fluorescence confirm that transgene expression following transduction of 293T cells is conditional on Cre activity.
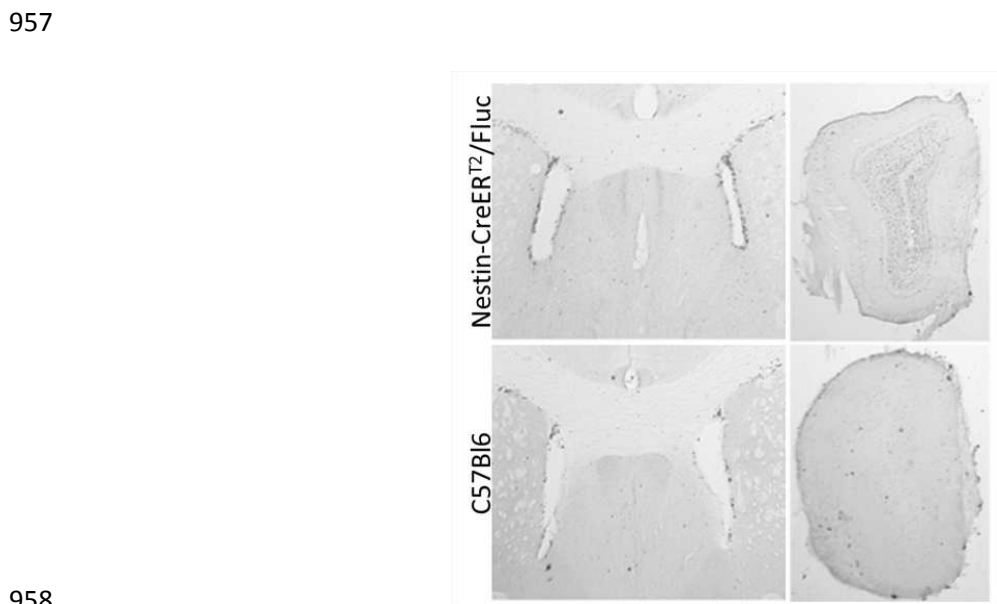

S Fig2. Neurogenic potential in Nestin-CreER[T2]/Fluc mice. BrdU staining of brain sections of the SVZ and OB of a Nestin-CreER[T2]/Fluc mouse (upper panel) compared to an age-matched C57BL/6 mouse (lower panel). BrdU was administered as previously published (Geraerts et al, 2006). There was no significant difference in the number of BrdU^{+} cells in both the SVZ (left) and OB (right) of Nestin-CreER[T2]/Fluc mice compared to C57BL/6 mice.

A

Contralateral side   Ipsilateral side

B

SVZ   stroke   stroke
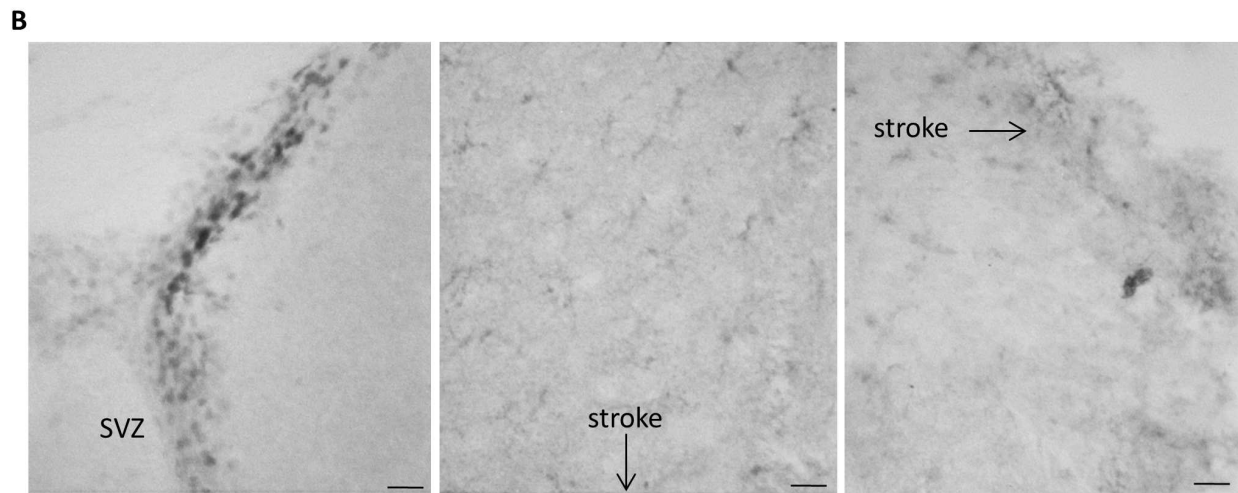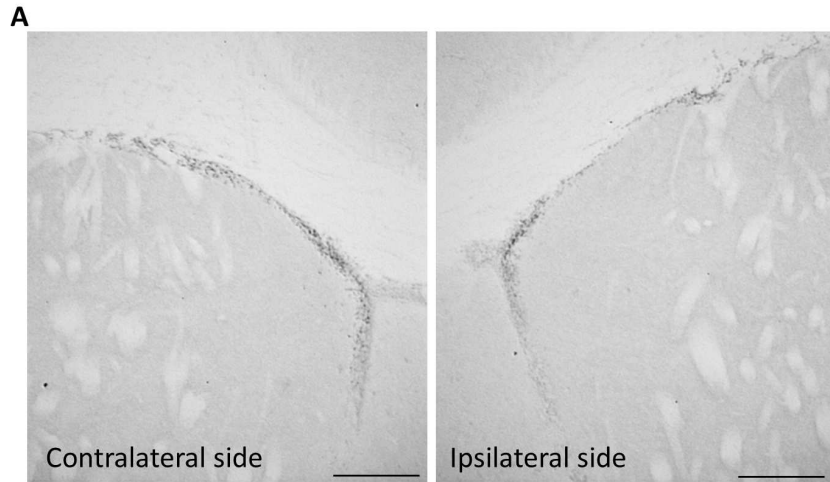
S Fig3. Upregulation of Cre expression near the stroke region. Cre staining of the SVZ, CC and stroke region at 2 days after stroke. (A) There were no major changes in Cre expression in the ipsilateral SVZ and CC in comparison to the contralateral hemisphere. (B) Cre expression in the ipsilateral SVZ (left panel), the cortex on the dorsal side of the stroke region (middle panel), the striatum on the lateral side of the stroke region (right panel). Cre expressing cells with astrocytic morphology were mainly detected in the cortex (middle panel). Scale bar (A) = 250 μm; (B) = 25 μm.

34

974
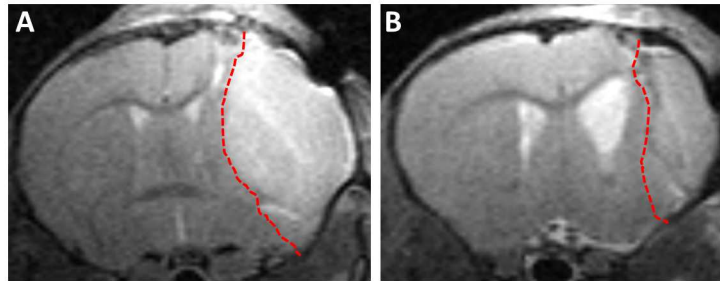
S Fig4. Anatomical changes in the brain of mice with PT stroke. (A) Representative T_2-weighted MRI of edema formation 2 days after stroke, at times resulting in a shift of the BLI signal towards the midline. (B) T_2-weighted MRI of an animal 14 days after stroke surgery with an enlarged ventricle in the ipsilateral hemisphere. The stroke regions in the right hemisphere are marked with a red dotted line.

980
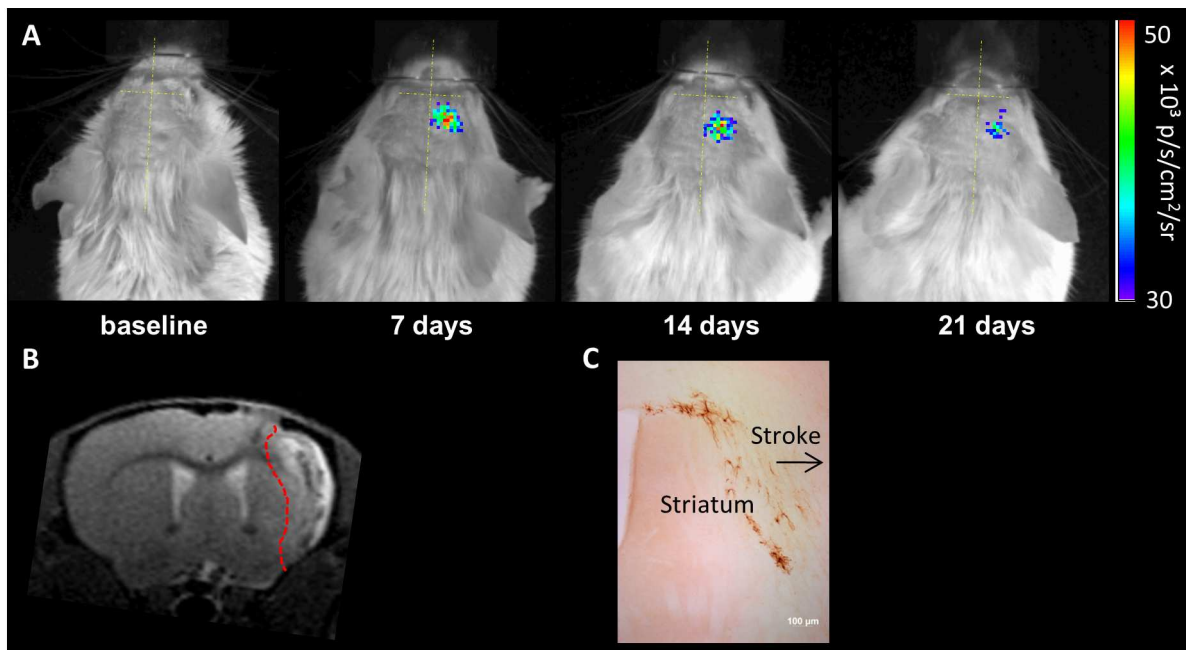
S Fig 5. Increased BLI signal in a Nestin-CreER^{T2} mouse after MCAO. (A) Nestin-CreER^{T2} mice were injected in the SVZ with the Cre-Flex LV. One week later, expression was induced by 5 days of tamoxifen treatment *via* oral gavage. 2 weeks after tamoxifen treatment, mice received MCAO or sham surgery. The mice were scanned prior to and 7, 14 and 21 days after stroke/sham surgery. This image represents the follow-up of a single mouse, showing a 5 fold increase in BLI signal after MCAO compared to baseline. This increase was detected in 1 out of 4 MCAO animals and was not observed in the sham-operated animals (n = 3). (B) This panel represents the corresponding T_2-weighted MR image of the animal depicted in (A) at 20 days after surgery. The stroke area in the right sensory motor cortex is marked with a red dotted line. (C) eGFP^{+} cells in the CC of the same animal 22 days after stroke.